CHARACTERIZATION OF CANINE MODELS OF ITCH AND CUTANEOUS INFLAMMATION IN ATOPIC DERMATITIS

By

Amanda Blubaugh

(Under the Direction of Frane Banovic)

ABSTRACT

Atopic dermatitis (AD) is a chronic pruritic and inflammatory skin disease with high prevalence that affects humans and dogs, with a majority of cases demonstrating IgE antibodies directed at environmental allergens. Canine and human spontaneous AD are often associated with diminished quality of life and an economic burden. Current murine models of AD lack high gene homology to human AD and have limited predictive power. The very near identical AD clinical phenotype between humans and dogs allows a unique opportunity to investigate both itch and inflammation in canine models for potential novel drug development benefiting one or both species. Using canine AD-like modeling and RNA sequencing techniques, we demonstrate high homology in immune and pruritogenic pathways between canine and human spontaneous AD. These observations will reveal that canine AD recapitulates molecular pathways in human AD and that those pathways are inducible in canine AD-like models for future investigation and therapeutic development.

INDEX WORDS: Canine, Human, Atopic, Atopic dermatitis, RNA sequencing, Transcriptome, Immunoglobulin-E, Late phase reactions, Chloroquine, Ethogram, Differential expression, Enrichment analysis, Spontaneous

CHARACTERIZATION OF CANINE MODELS OF ITCH AND CUTANEOUS INFLAMMATION IN ATOPIC DERMATITIS

By

Amanda Blubaugh

B.S., Georgia Southern University, 2010

A Dissertation Submitted to the Graduate Faculty of the University of Georgia in Partial Fulfillment of the Requirements for the Degree

DOCTOR OF PHILOSOPHY

ATHENS, GEORGIA, UNITED STATES

2024

CHARACTERIZATION OF CANINE MODELS OF ITCH AND CUTANEOUS INFLAMMATION IN ATOPIC DERMATITIS

By

Amanda Blubaugh

Major Professor:	Frane Banovic
Committee:	Shaying Zhao
	Robert M. Gogal Jr
	Elizabeth Howerth

Electronic Version Approved:

Ron Walcott
Vice Provost for Graduate Education and Dean of the Graduate School
The University of Georgia
May 2004

DEDICATION

For all those deeply in need of a voice, but with none to convey their needs.

For Michael Blubaugh, who has been an unwavering support for all the years leading up to and through this endeavor.

For my entire family, particularly my mother, father, sister, and in-laws who have always guided me to believe in myself and push myself to be the best person I could be. I am who I am because of you.

For veterinary technicians and nurses like Billie Walker, Lynn Reece, Tara Denley, and Kathy Hoover, who continue to inspire me and allow me to learn from their experiences, who have been an invaluable resource throughout my development as a veterinary nurse, on my way to becoming a veterinarian, and through my passion to be a researcher.

For every client of every dog like Turner, willing to undergo biopsy of their skin to contribute to this field; may they and theirs benefit from the advances made by these studies through treatments created because of them. Each transcriptomic thumbprint, each histologic visualization of cellular influx to this immunologically active area of the body provides another perspective for the best picture of the disease.

For dogs especially like Gretchen, who developed my appreciation for MRSP, skin grafts, skin healing, dermatology in general, and in how an immunological organ like the dermis is often overlooked, lost for the trees by lymph nodes, gut mucosa, immunologically privileged sites, and all other specialized tissues (there are so many of them). For all the dogs, and humans, I have met struggling with these issues; there are so many of you.

ACKNOWLEDGEMENTS

I would like to thank from the bottom of my heart all the supporters and role models I have had through this journey. For Drs Tiffany McAllister, Janice Grumbles, and Hiro Iwamoto, who believed in my potential as a veterinarian to impact change and supported my dreams.

A huge thank you to Dr. Frane Banovic, a superb mentor in the field and in life.

Great thanks to Drs Buffy Howerth, Bob Gogal, and Shaying Zhao, as well as Walt Lorenz, for their support in these studies and their guidance and time as part of my committee.

A special thank-you to Boehringer Ingelheim for funding vital research and supporting young researchers in the veterinary field. Your contributions to the betterment of animal and human lives through such support are not forgotten.

TABLE OF CONTENTS

LIST OF TABLES

Page

LIST OF FIGURES

Page

CHAPTER 1

INTRODUCTION

Atopic dermatitis, or eczema, is a common disease that affects up to 20% of the human and canine populations (Marsella and De Benedetto, 2017; Olivry, 2012). In both species, the pathogenesis of AD is thought to involve a complex interaction of genetic, immune, and environmental factors leading to immune dysregulation and skin barrier dysfunction (Hensel et al., 2024; Santoro et al., 2024). Pruritus is considered the cardinal symptom of AD in both species, frequently leading to low quality of life. Currently, none of the treatments are able to resolve and cure AD in humans and dogs and the majority of patients require long-term medical management to control the disease (Santoro and Marsella, 2014). Murine models of AD have been used for decades to decipher the pathogenesis of human AD. Interestingly, dogs develop spontaneously AD with nearly similar clinical phenotypes as observed in humans with AD (Marsalla, 2009). Furthermore, canine AD models, such as house dust-mite sensitized dogs and IgE-mediated reactions, are commonly used to evaluate novel treatments in preclinical trials.

Gene expression profiling of inflammatory skin diseases has been widely used to identify gene alterations in lesional and non-lesional skin compared to healthy skin in order to understand the molecular fingerprint, define pathogenic immune pathways, and identify disease-specific biomarkers for treatment. There has been a substantial amount

of research into the molecular features of human AD (Nomura et al., 2018; Steinhoff et al., 2022; Tsoi et al., 2019; Tsoi et al., 2020). However, it is currently unknown whether spontaneous canine AD skin lesions and canine IgE-mediated AD model reactions molecularly resemble spontaneous human AD.

The interleukin 31 (IL-31)-induced canine pruritus model has been used as the sole itch model in dogs to evaluate novel treatments such as JAK-STAT inhibitors and anti-IL31 monoclonal antibodies (Gonzales et al., 2016; Gonzales et al., 2013). Several investigations of other itch-inducing compounds in humans and mice have not resulted in significant upregulation of pruritus in dogs. Chloroquine (CQ) is a prototypical systemic and intradermal pruritogen for histamine-independent (nonhistaminergic) itch in mice and humans (Ajayi, 1989; Tarrasón, 2017). A recent single publication showed promising pruritic responses after CQ administration to healthy research dogs, however, the predictive validity of this model is poorly understood in dogs and requires in-depth investigation (Aberg et al., 2015).

The main objectives of the present studies were to characterize the transcriptomic profiles of canine AD-like models and determine how closely they resemble the phenotypic and molecular abnormalities observed in canine and human spontaneous AD skin. Furthermore, we attempted to develop the canine model for non-histaminergic itch and cutaneous inflammation by using the pruritogen chloroquine.

The objectives and hypotheses examined in this thesis are summarized below:

Objectives

1. To define the transcriptome (gene expression profiling) of the canine IgE model of atopic dermatitis (AD) by:
    a. Characterizing the inflammatory and pruritogenic transcriptome of experimental acute canine IgE-induced lesions following intradermal injection of anti-immunoglobulin E (IgE) antibodies in healthy dogs using RNA-sequencing.
    b. Downloading and re-analyzing available human published datasets available through the Gene Expression Omnibus (GEO) repository (http://www.ncbi.nlm.nih.gov/geo), a public gene-related database, and using the following selection criteria:

       (1) the study should contain expression data of normal skin biopsy and acute AD (e.g., lesion developed in less than 72-hr duration, lack of skin lichenification and histopathologic features of chronic AD lesions)) lesional skin biopsies without any immunomodulatory drugs provided to patients at the time of biopsy (i.e. to avoid potential effect of drugs); (2) samples should be from humans (*Homo sapiens*); and (3) the transcriptome expression profiling by RNA-seq should be ≥75 paired end base pair reads so it can be compared to the sequencing platform performed in this study.
    c. Comparing this transcriptome data to acute human AD lesions to evaluate overlap and correlations with strict Differentially Expressed Gene (DEG)

cutoffs and subsequent Spearman correlations, pathway analyses, and Gene Set Variation Analyses (GSVA).

d. Correlating findings of RNA-sequenced acute canine IgE-induced lesions after intradermal injection of anti-immunoglobulin E (IgE) antibodies in healthy dogs to that of the Global Wheal Scoring (GWS) performed on induced lesions.

2. To perform comparisons of global transcriptome profiles of skin lesions and correlation of spontaneous human and canine AD by:

   a. Characterizing the inflammatory and pruritogenic transcriptome of spontaneous canine AD lesional (AL), and non-lesional (ANL) to healthy (NN) skin using RNA-sequencing.

   b. Downloading and re-analyzing human published datasets available in the through the Gene Expression Omnibus (GEO) repository (http://www.ncbi.nlm.nih.gov/geo); part of the Sequence Read Archive (SRA) of the National Center for Biotechnology Information (NCBI) from the National Institutes of Health (NIH) National Library of Medicine after performing a cross search of qualified datasets with the same selection criteria from objective 1.

   c. Using this published and analyzed cohort data of the lesional human AD transcriptome to identify correlations between human and canine spontaneous AD in similar fashion to those correlations found between human atopic dermatitis and anti-canine-IgE mediated lesions from objective 1.

3. To develop a canine histaminergic-independent itch model using CQ (chloroquine) through determination of pruritogenic and inflammatory effects of systemic and intradermal CQ injections in healthy dogs.by:
    a. Developing an ethogram; a methodology to quantify systemic pruritus in dogs for canine pruritic behaviors and by scoring systemic and local itch behaviors using blinded video-recordings.
    b. Characterizing intradermal CQ provoked global wheal scores in healthy canine skin for corroboration of inflammatory changes to those pruritic behaviors recorded.
    c. Evaluating the pruritic effects and global wheal scores (GWS) in contrast between a vehicle (buffered saline) and CQ to determine the significance of CQ's effects.

Hypotheses

Our central hypothesis was that the transcriptomic profiles of canine AD-like models and spontaneous canine AD would closely resemble the phenotypic and molecular abnormalities observed in human spontaneous AD skin. Furthermore, we hypothesized that we would be able to develop a canine model for non-histaminergic itch and cutaneous inflammation by using the pruritogen chloroquine. Our individual hypotheses were that:

1. Significant variations will exist in cellular infiltration and expression of immune and barrier genes between anti-canine-IgE, saline control, and healthy skin lesions.
2. Evaluation of anti-canine-IgE-mediated lesions via the RNA-seq transcriptome will show mediation of similar T-helper pathways and barrier changes to that of acute spontaneous human AD lesions.
3. IL-13 would represent the dominant Th2 cytokine in the anti-canine IgE model similarly to spontaneous human atopic dermatitis, and that this would aid in the development of screening experimental models for studying the anti-inflammatory effect of anti-allergic drugs before entering clinical trials.
4. The transcriptome of spontaneous canine AD skin will exhibit a striking similarity to human AD regarding changes in activation of T helper cell gene markers and shared differentially expressed genes (DEGs) using Spearman correlation; IL-13 would be the dominant cytokine.

5. CQ injections will induce acute inflammation in healthy dogs, and that this could be measurable via ethogram and Global Wheal Score (GWS) evaluation by developing a methodology to quantify systemic pruritus in dogs for canine pruritic behaviors and by scoring systemic and local itch behaviors using blinded video-recordings.
6. Further, a developed ethogram evaluation of this kind could be applied to other pruritic behavior studies for future canine pruritic models of acute inflammation for atopic dermatitis.

CHAPTER 2

LITERATURE REVIEW TO ATOPIC DERMATITIS AND ITS CURRENT CANINE MODELS

Atopic dermatitis

Canine atopic dermatitis (AD) is a highly pruritic and inflammatory skin disease; it is estimated that that AD affects over 10% of the canine population with a majority of cases demonstrating IgE antibodies directed at environmental allergens (Olivry et al., 2015). In the human population, up to 20% of individuals have a moderate to severe AD that encompasses similar chronic hypersensitivity, pruritus, inflammation, and need for continuous medical management as seen in dogs (Hamilton et al., 2014; Santoro and Marsella, 2014). Canine and human AD are often associated with diminished quality of life and an economic burden (Bieber et al., 2017; Gittler et al., 2013; Lourenco et al., 2016).

Treatment with allergen immunotherapy (AIT) is considered the only curative measure, but it does not work in every patient. A good success rate between 57% to 70% is observed in AD dogs (Plant and Neradilek, 2017), with many dogs requiring concurrent systemic immunomodulating drugs with AIT (Marsella and De Benedetto, 2017). The main disadvantage of AIT is the duration to effect; usually it requires up to three years to achieve its effects and symptomatic therapy is needed in the meantime (Lee et al., 2015). Finally, AIT is often presented as an expensive option for clients because of the initial high costs for testing and formulation of AIT (Marsella and De Benedetto, 2017).

Treatment of severe and chronic canine AD cases can be challenging, commonly requiring topical and systemic agents. Systemic immunosuppressants such as glucocorticoids, cyclosporine, and oclacitinib have been used for long-term control of refractory patients with recurrent flares (Olivry et al., 2015). More recently, lokivetmab once monthly injectable therapy, a monoclonal antibody against cytokine interleukin 31 (IL-31), has been shown to reduce pruritus and partial clinical signs in canine AD (Marsella and De Benedetto, 2017). Lokivetmab can be used for long-term symptomatic AD control as well, however, the effect appears stronger in mild versus moderate to severe AD dogs.

Patho-mechanisms of human AD

The genomics revolution has greatly contributed to our knowledge of human AD. The initial studies reported microarray-based transcriptome profiles obtained from biopsies of visibly lesional or non-lesional human AD skin (for example in (Esaki et al., 2015; Gittler et al., 2013; Gittler et al., 2012; Saaf et al., 2008; Suarez-Farinas et al., 2013a; Suarez-Farinas et al., 2011)). These studies have provided relevant insight on the inflammatory and structural changes occurring at the time of acute or chronic AD skin lesions, or after immunomodulating treatment with cyclosporine (Rozenblit et al., 2014), narrow-band UVB (Suarez-Farinas et al., 2013b) or the monoclonal IL4/IL13 antibody dupilumab (Hamilton et al., 2014). Ultimately, Th2, Th17, and Th22 cell types have all been shown to contribute to AD pathogenesis through the demonstration of suppression in their activation after broad, systemic treatment of the disease in humans (Esaki et al., 2016).

Small sample sizes and microarray analysis have still limited coverage to detect all genes and low-expressed transcripts (Suarez-Farinas et al., 2015; Tsoi et al., 2019). Recently, transcriptome studies based on RNA-sequencing (RNA-seq) have been instrumental to identify key transcripts and pathways in human AD skin lesions, establishing dominance of IL-13 pathways (Bieber, 2020; Tsoi et al., 2019) in the Th2 response, which has concordantly been documented in quantitative or real-time polymerase chain reactions (qPCR, rtPCR) in both children and adults (Esaki et al., 2016), and has been acknowledged as difficult in detection on microarrays (Suarez-Farinas et al., 2015). RNA-seq allows analysis of the entire genome compared to the limitations of genes in microarray analysis; these newer technologies have begun to unravel the multipolar T helper (Th) cell axis pathogenesis involved in AD that reflects the heterogeneity of the disease (Suarez-Farinas et al., 2015; Tsoi et al., 2019).

Unfortunately, the main limitation of these more recent studies is the inability to evaluate the dynamics and fluctuations of the AD lesions, as one cannot precisely assess the age of biopsied skin lesions in patients with spontaneous AD clinically. In a recent study by Tsoi et al (2021), only lesions known to be over 72 hr in age were collected to prevent spontaneous acute and subacute lesional samples from interfering with lesional profiling of chronic AD.

Patho-mechanisms of canine AD

Studies of the canine spontaneous AD transcriptome have still been limited to two microarray studies. While revealing many genes differentially expressed in canine AD

skin (Plager et al., 2012; Wood et al., 2009), the lack of key epidermal barrier and inflammatory cytokine genes in the microarrays has inhibited discussion toward specific immunologic changes.

Canine microarrays with limited numbers of genes were necessary previously due to cost limitations of RNA-seq; however, costs have declined greatly in the advent of technological improvement (Hofker et al., 2014). Further, RNA-seq has since been shown to improve 13-18% in accuracy in determining differentially expressed genes (DEGs), especially with low abundance transcripts, when compared to microarrays and verifying DEG expression with qPCR (Suarez-Farinas et al., 2015; Wang et al., 2014).

In a recent canine AD microarray study by Plager et al (2012), IL4 and IL13 cytokines were not available in the probe set for identifying the Th2 polarized profile of canine AD, although the authors did a superb job of identifying differentially expressed genes that indicate IL4 and IL13 involvement in the disease (e.g., ARG1, CCL2, and CCL17). Antimicrobial S100 proteins were included in the probe set and found to be increased in expression in lesional samples compared to healthy canine tissue, enforcing antimicrobial peptide increased activity previously found in human lesional AD (e.g., S100A8, S100A9, S100P, S100A3) associated with skin barrier disruption. However, Th22-associated epidermal barrier (IL22) and certain inflammatory gene markers (e.g., LTB, IL18) were not identified. This further highlights the disadvantages of microarray use, as probe set microarrays that included these markers and further dissected the skin into epidermal and dermal layers for increased sensitivity in other human atopic studies were able to identify increased expression in AD lesional skin (Esaki et al., 2015).

Pruritus in murine models of AD and spontaneous human and canine AD

Pruritus in human AD has been extensively investigated (Ajayi, 1989; Furue and Kadono, 2015; Mollanazar et al., 2016; Yosipovitch et al., 2018), particularly with the use of murine models (Akiyama et al., 2010; Foroutan et al., 2015; LaMotte et al., 2011; Liu et al., 2009; Tarrasón, 2017). Multiple factors, including proteases and their receptors (PARs) have been investigated as AD studies have found upregulation of these in patient skin (Akiyama et al., 2015). Other investigations have focused on algesic (algogens such as capsaicin) and other chemical (such as the anti-malarial chloroquine) stimuli to determine mechanisms of itch outside of classically defined histaminergic itch (Akiyama et al., 2010; LaMotte et al., 2011; Liu et al., 2009).

Modelling itch in canines has proven more difficult compared to mice, and fewer studies have been published on the topic (Aberg et al., 2015; Carr et al., 2009; Gonzales et al., 2016; Olivry, 2017; Olivry et al., 2013; Osifo, 1991; Paps et al., 2016). Homologies regarding the induction of itch have already been investigated: for instance, cowhage-inducing itch in dogs mirrors identified PAR activation and itch by cowhage in humans (Akiyama et al., 2015; Olivry et al., 2013). Other parallels have yet to be explored. For example, while thymic stromal lymphopoetin (TSLP) has been identified in humans (and mice) to be a pruritogen through direct afferent nerve terminal receptor presence and induction of itch (Turner and Zhou, 2014; Wilson et al., 2013), no studies have yet evaluated TSLP-itch inducing effects in dogs. Clinical trials have previously focused on the treatment of itch in canines with histamine 1 receptor (H1R) inverse agonists

(antihistamines) with no benefit (Furue and Kadono, 2015; Mollanazar et al., 2016; Olivry, 2017), underlining the need to unravel other potential pruritic pathways for targeted therapy.

Murine and Canine AD-like models

An ideal model for AD has continually been sought after in murine and canine models. Classic murine models of AD are generally induced through epicutaneous sensitizer application (hapten induction), transgenic models targeting specific molecule selection (genetically engineered knockout mice), or spontaneous skin lesion strains (such as NC/Nga mice) (Martel et al., 2017). The Flaky Tail mouse ($Matt^{ma/ma}$ $Flg^{ft/ft}$) is worth noting, as a mutation in the filaggrin and matted genes allows spontaneous AD lesions to develop (Rerknimitr et al., 2017). Other murine models of interest include the IL-4 and TSLP transgenic mice, whose pruritus and dermatitis was found to correlate to IgE and IgG1 elevations and whose inducible skin-specific TSLP allowed erythema and progressive similar AD symptoms within weeks, respectively (Jin et al., 2009). Recent transcriptome comparison between murine models of AD and human AD have provided a deeper understanding of the complex molecular networks between species (Esaki et al., 2016; Ewald et al., 2015; Martel et al., 2017). The maximum overlap of genes between murine AD-like models and human AD specific gene lists (meta-analysis derived AD: “MADAD”) remained under 40%, which explains the limited predictive power of murine preclinical AD-like models for humans (Ewald et al., 2015). Canine AD-like models (house-dust mite-induced and IgE models) are used to simulate canine AD for preclinical assessments and treatments; however, their comparative transcriptomic profiles with canine and human spontaneous AD have not been well characterized.

Current canine AD-like models used include house dust mite (HDM; *Dermatophagoides farinae* spp.) model in sensitized dogs and the IgE model in healthy dogs. Both models induce acute lesions that can be studied over a 48-72 hr period. The HDM model is characterized by epicutaneous application of HDM slurry on the skin, whereas the IgE model features intradermal injections of rabbit or goat anti-IgE injections. All canine AD-like models have been used for decades to evaluate novel drugs and therapeutics without studying their molecular networks and mechanisms and their overlap to canine spontaneous AD or comparison to human spontaneous AD. Dogs are the closest animal to naturally develop AD outside of humans and the only animal to resemble human AD so closely in etiology. Thus, the development of AD models in canines appears imperative for translational medicine (Santoro and Marsella, 2014).

In 2006, the canine IgE AD-like model was studied by Pucheau-Haston et al. using qPCR, histological, and immunohistochemical staining. Intradermal injection of anti-canine-IgE in normal dogs resulted in a rapid biphasic influx of inflammatory cells, with early influx of predominantly activated eosinophils, mast cells, and neutrophils, whereas mainly T-cells and dendritic cells predominated at 24 hr (Pucheu-Haston et al., 2006). The study showed upregulation of IL-13 in the IgE-mediated skin lesions. Furthermore, it demonstrated suppression of IL-13 and reduction of cellular infiltrate using prednisolone administration, but the sample size was too low to reveal any significance. Currently, in-depth investigations of IgE-mediated skin transcriptome in dogs are lacking.

Only recently, a microarray-based transcriptome investigation of HDM skin lesions following topical epicutaneous application revealed activation of innate and adaptive immune responses and pruritogenic pathways (Olivry et al., 2016). This study consisted of an extensive probe set for the microarray, allowing for the identification of multiple associated genes that were previously limited in discovery with other canine microarray studies (Plager et al., 2012; Schamber et al., 2014). The study revealed that acute HDM skin lesions feature upregulation of Th2 cytokines IL-4, IL-5, IL-13, and IL-31, as well as IL33. IL22, as a part of the Th22 pathway, was also shown to be upregulated in the acute canine HDM lesion. The main limitation of this study was the control group, as saline was used for control instead of healthy skin samples. Furthermore, the transcriptome data analyzed using microarray may not have revealed all changes as possible with RNA sequencing.

CHAPTER 3

CHARACTERIZATION OF THE PRO-INFLAMMATORY AND PRURITOGENIC TRANSCRIPTOME IN SKIN LESIONS OF THE EXPERIMENTAL CANINE ATOPIC ACUTE IGE-MEDIATED LATE PHASE REACTIONS MODEL AND CORRELATION TO ACUTE SKIN LESIONS OF HUMAN ATOPIC DERMATITIS[1]

[1]Blubaugh, A; Hoover, K; Kim, SJ; Fogle, JE; Banovic, F. 2024. *Veterinary Sciences*. 11(3): 109. https://doi.org/10.3390/vetsci11030109.

Reprinted here with permission of the publisher.

Abstract

Intradermal injection of anti-immunoglobulin E (IgE) antibodies in dogs grossly and histologically resemble naturally occurring atopic dermatitis (AD). However, the activated inflammatory and pruritic pathways have not been characterized. The objectives of this study were to characterize the inflammatory transcriptome of experimental acute canine IgE-induced lesions and to determine how this correlates to the transcriptome of naturally occurring human and canine acute atopic dermatitis. Biopsies were collected at 6 and 24 h after intradermal injections of anticanine-IgE antibodies to eight healthy male castrated Beagles; healthy and saline-injected skin served as controls. We extracted total RNA from skin biopsies and analyzed transcriptome using RNA-sequencing. Gene expressions of IgE-induced biopsies were compared to that of controls from the same subject (1.5-fold change, P-adjusted value $\leq$ 0.05). Acute IgE-mediated lesions had a significant upregulation of pro-inflammatory (e.g., LTB, IL-1B, PTX3, CCL2, IL6, IL8, IL18), T helper-(Th)1/IFNγ signal (e.g., STAT-1, OASL, MX-1, CXCL10, IL-12A) and Th2 (e.g., IL4R, IL5, IL13, IL33 and POSTN) genes, as well as Th2 chemokines (CCL17, CCL24). Pathway analysis revealed strong significant upregulation of JAK-STAT, histamine, IL-4 and IL13 signaling. Spearman correlation coefficient for the shared DEGs between canine anti-canine-IgE and human AD samples revealed a significant moderate positive correlation for anti-canine-IgE 6-hr samples (r=0.53) and 24-hr samples (r= 0.47). In conclusion, acute canine IgE-mediated skin lesions exhibit a multipolar immunological axis upregulation (Th1, Th2 and Th17) in healthy dogs, resembling acute spontaneous human AD lesions.

Introduction

Atopic dermatitis (AD) is a pruritic, recurrent and chronic inflammatory skin disease, frequently associated with elevated systemic immunoglobulin-E (IgE) levels, that spontaneously develops in humans and dogs (Marsella, 2021). In both species, the pathogenesis of AD is thought to involve a complex interaction of genetic, immune and environmental factors leading to immune dysregulation and skin barrier dysfunction (Marsella, 2021).

Immunoglobulin-E plays a role in allergen-induced inflammatory processes in atopic subjects via preformed allergen-specific IgE molecules bounded to the high-affinity IgE receptors (FcεRI) on the surfaces of various immune cells (Clark, 1989; Wollenberg et al., 2021). By binding with incoming allergens, IgE acts as an effector for activation of immune cells, chemical mediator release and cytokine/chemokine production.

Intradermal injection of anti-canine-IgE in healthy dogs results in immediate and late-phase reactions (LPR); LPRs follow 3 to 48 hr after allergen challenge and are accompanied by inflammatory cell infiltration that histologically resembles changes seen in naturally occurring canine atopic dermatitis (Olivry et al., 2001; Pucheu-Haston et al., 2006). Therefore, cutaneous IgE-mediated LPRs have been used as a screening atopic dermatitis model for studying the anti-inflammatory effect of anti-allergic drugs before entering clinical trials (Baumer et al., 2017; Bizikova et al., 2010; Blubaugh et al., 2018; Pucheu-Haston et al., 2014). Interestingly, a pilot quantitative reverse-transcription PCR analysis of canine IgE-mediated LPRs with only a few genes investigated revealed

increased expression of proallergic cytokine interleukin-13 (IL-13) and CC chemokine ligand 5 (CCL5) and CCL17 (Pucheu-Haston et al., 2006). However, to the best of the authors' knowledge, there have been no evaluations of activated inflammatory and pruritic molecular pathways in IgE-mediated cutaneous LPRs of healthy dogs (Bieber, 2014).

Given that emerging novel AD treatments are designed to target specific inflammatory mediators or pruritogens, it is imperative to understand the molecular signature of the pre-clinical AD models in humans and dogs. In the past decade, the molecular signatures of numerous human inflammatory skin diseases have been evaluated using gene expression microarrays, which contain limited number of genes for analysis. Currently, RNA-sequencing (RNA-seq) is commonly used for the evaluation of molecular signatures in skin diseases as it provides the analysis of whole transcriptome and avoids technical issues with microarray (e.g., probe performance).

In this study, we characterized the activation of early immunologic and pruritogenic pathways in experimental canine acute IgE-mediated LPR model using RNA-seq of skin biopsy samples sequentially obtained after anti-IgE intradermal injections. Furthermore, we searched through the published RNA-seq databases for acute spontaneous human and canine AD skin biopsies datasets with the goal of performing a comparative analysis of the differentially expressed genes (DEGs) and transcriptional pathways between acute canine IgE-mediated LPR model and acute spontaneous AD data.

Materials and Methods

2.1. Patient inclusion

Eight clinically healthy male castrated research beagle dogs (age 2-3 years) with no previous history of pruritus or skin disease were included in this study. The dogs were housed in the laboratory animal facilities at the university setting under conditions compliant with laboratory animal requirements. All aspects of the study were conducted in accordance with the Institutional Animal Care and Use Committee.

2.2. Intradermal injections and skin biopsy collection of late phase reactions (LPRs)

The IgE-mediated LPRs model was performed as previously described (Pucheu-Haston et al., 2006) (Supplementary Material 1). Dogs were sedated intravenously using medetomidine (Domitor, Pfizer, Exton, PA) and baseline healthy skin biopsies were obtained 7 days before the anti-IgE/control intradermal injections. Two intradermal injections of 0.05 mL of anti-canine-IgE polyclonal antibodies (0.08 mg/mL, goat anti-canine IgE AHP946, Bio-Rad Laboratories, Inc., Hercules, CA, USA) and 0.05 mL phosphate-buffered saline (diluent, negative control; Sigma-Aldrich, St Louis, MO, USA) were administered on one side of the thorax and blindly evaluated by an investigator (FB); histamine (0.1 mg/mL, Sigma-Aldrich) served as a positive control.

The order of injections was randomized for every dog using statistical computer software (GraphPad Prism 8.0) and the investigator (FB) was blinded during intradermal

injection evaluations. Clinical scoring by blinded investigator (FB) involved a global wheal score (GWS) and LPRs (Bizikova et al., 2010; Pucheu-Haston et al., 2006).

Skin biopsy samples were collected from IgE-mediated cutaneous reactions at 6- and 24-hr post-injections; the 6- and 24-hr saline sample served a s negative control. All biopsies were bisected; one half was placed in neutral buffered formalin, and the other was immersed immediately in RNALater and kept frozen until RNA extraction.

2.3. Histopathology

Five-micrometer paraffin-embedded sections were stained with haematoxylin and eosin for examination of inflammatory cells. All slides were evaluated by a board-certified pathologist and the results were expressed as a number of positively staining cells in superficial dermis per 10 consecutive 40X high power fields (HPF), excluding endothelial cells and adnexa.

2.4. RNA-sequencing analysis

The sample size for RNA-seq was determined to be sufficient to provide at least 80% power to detect a significant 1.5-fold difference in values (mRNA transcription) between pre- and post-injections skin biopsy samples using ssizeRNA (Baumer et al., 2017). Total mRNA was extracted using miRNAeasy kit from Qiagen (Qiagen, Valencia, CA) following the manufacturer's specifications. Only samples with a 260/280 ratio of ~1.8-2.0 (RNA) and showing a ribosomal integrity number (RIN) above 7 were subjected to further library preparation and sequencing. Forty RNA samples were analyzed in this

study: eight healthy non-treated skin samples, eight samples from 6 and 24 hr post-intradermal saline (control) and eight samples from 6 and 24 hr post-intradermal anti-IgE injection. Sequencing was performed on NovaSeq 6000 with 150 paired-end base pairs (32 samples) and with the NextSeq 2000 with 75 paired-end base pairs (8 samples) according to the manufacturer's protocol (Illumina, San Diego, CA). For RNA-seq data analysis, please see Supplementary Material 1.

2.5. Quantitative reverse-transcription PCR analysis

To confirm the gene expression results from RNA-seq data in this study, Quantitative real-time polymerase chain reaction (qRT-PCR) was performed for anti-canine IgE skin reactions at 6- and 24-hr timepoints for selected genes. Expression of CCL2, C-X-C motif chemokine ligand 10 (CXCL10), CCL17, IL-1B, tissue necrosis factor alpha (TNF-α) and IL-33 was measured by quantitative reverse-transcription PCR (qRT-PCR; see Supplementary Material 1).

2.6. Correlation analysis to previously published transcriptome data using RNA sequencing for acute skin lesions in human and canine atopic dermatitis

To assess the molecular similarity of canine IgE-mediated LPRs and acute lesions of human/canine spontaneous AD skin, Gene Expression Omnibus (GEO) repository (http:// www.ncbi.nlm.nih.gov/geo), a public gene-related database was searched for original RNA seq expression data for human and canine acute atopic dermatitis using the following selection criteria: (1) the study should contain expression data of normal skin biopsy and acute AD (e.g., lesion developed in less than 72-hr duration, lack of skin

lichenification and histopathologic features of chronic AD lesions)) lesional skin biopsy without any immunomodulatory drugs provided to patients at the time of biopsy (i.e. to avoid potential effect of drugs); and (2) samples should be from Homo Sapiens and Canis lupus; and (3) the transcriptome expression profiling by RNA-seq ≥75 paired end base pairs reads so it can be compared to the sequencing platform performed in this study.

Correlation between significantly upregulated/downregulated DEGs (FC= +/- 1.5; FDR<0.05) of anti-canine-IgE reactions at 6- and 24-hr and spontaneous human and canine AD acute lesional skin specimens was evaluated using Spearman correlation coefficients on log2-transformed levels as previously described. Data were presented in scatterplots with estimated linear regression and a 95% confidence interval.

2.7. Statistical and bioinformatics analyses

Results of the clinical evaluation (GWS and GLS), as well as cell counts for each time point, were compared with using nonparametric repeated measures one-way ANOVA (Friedman test) with a level of significance set at $P < 0.05$. Normalization of RNA-seq data and DE analysis between different conditions (e.g., healthy, control, IgE, atopic lesional) was performed using empirical Bayes linear model, DESeq2, as implemented through the vignette (Love et al., 2014). A false discovery rate (FDR) of less than 0.05 and fold change (FC) of +/- 1.5 or greater was used to determine differentially expressed genes (DEGs). Phenotypically unbiased evaluation of gene set variation between groups was performed with Gene Set Variation Analysis (GSVA) (Hanzelmann,

2015; Ritchie et al., 2015). Functional enrichment analysis for pathway identification was done using the Metacore platform for all DEGs (Freudenberg et al., 2019; Metacore, 2023).

Results

3.1. Global wheal score, late phase reaction scores and histopathological examination

Intradermal injections of anti-canine-IgE and histamine resulted in positive wheal and erythema reactions on the thorax in all eight dogs (Figure 1.1a,c). There were no wheal and flare reactions observed after the intradermal injections of phosphate-buffered saline (control, Figure 1.1a). Anti-canine-IgE injections induced significant LPRs at 6 (Wilcoxon matched-pairs signed-rank test, P=0.007 for saline, P=0.005 for histamine) and 24 (P=0.044 for saline, P=0.044 for histamine) hr, compared to phosphate-buffered saline and histamine (Figure 1.1b,d), respectively. A blinded histological evaluation of 6- and 24-hr anti-IgE-associated LPRs revealed a significant increase in total leukocyte superficial dermal cell infiltrate (Figure 1.1e; P=0.041 for 6-hr, P=0.003 for 24-hr), as well as lymphocyte (Figure 1.1g; P=0.022 for 6-hr, P=0.007 for 24-hr), counts compared with corresponding saline timepoints. Elevated eosinophil numbers were observed in 6- and 24-hr IgE-mediated LPRs, but a significant increase was only identified in 24-hr IgE LPRs (Figure 1.1f; P=0.011, respectively).

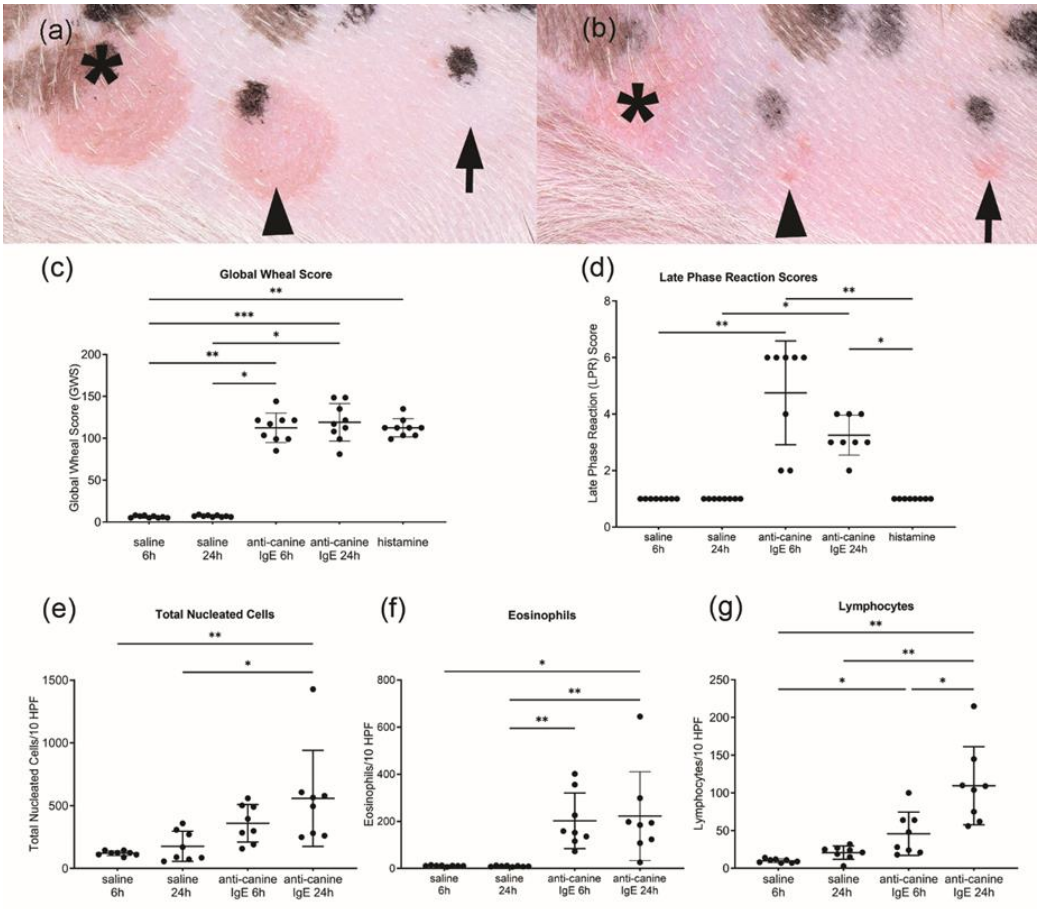

Figure 1.1. Clinical images of wheal and flare responses after 20 min (GWS; a) and 6 hr (LPRs, b) of injected compounds anti-canine IgE (asterisk), histamine (arrowhead) and phosphate-buffered saline (arrow). Anti-canine-IgE injections induced strong global wheal scores (GWS; c) and late phase reactions (LPRs; d) at 6- and 24-hr, compared to phosphate-buffered saline and histamine control. (e, f, g) Histopathological evaluation of the number of inflammatory infiltration cells (e), eosinophils (f) and lymphocytes (g) in saline and anti-IgE late phase reactions (LPRs). *p-adj < 0.05, **p-adj < 0.01, ***p-adj < 0.005.

3.2. RNA-seq molecular profiling of anti-canine-IgE- and saline-mediated late phase reactions (LPRs)

Using criteria of fold change/FC of +/- 1.5 and false-discovery rate/FDR <0.05 to define differentially expressed genes/DEGs, we identified 5042 (6 hr; 2481 up- and 2561-downregulated) and 3551 DEGs (24 hr; 1970 up- and 1581-downregulated) in anti-canine IgE groups versus healthy normal skin. In contrast, saline injections induced lower number of DEGs at 6 (total 1540; 775 up- and 764-downregulated) and 24 (total 1152; 591 up- and 561-downregulated) hr compared to normal skin. A principal component analysis (PCA), as depicted by the fitted ellipses, demonstrates separation within each group and clear deviation of groups between healthy, saline, and IgE at the 6- and 24-hr timepoints after batch correction and normalization (Supplementary Figure S1.1).

Overall, both injections (anti-canine-IgE and saline) induced significant differences in treated versus healthy skin for numerous immune genes, with anti-canine-IgE-induced lesions generally producing stronger immune responses (Figure 1.2, Supplementary Table S1.1). These include significant upregulations of pro-inflammatory (IL-1β, IL-8/CXCL8, IL-6, IL-18) and Th1 (CXCL10, STAT1, MX1, CCL4) markers.

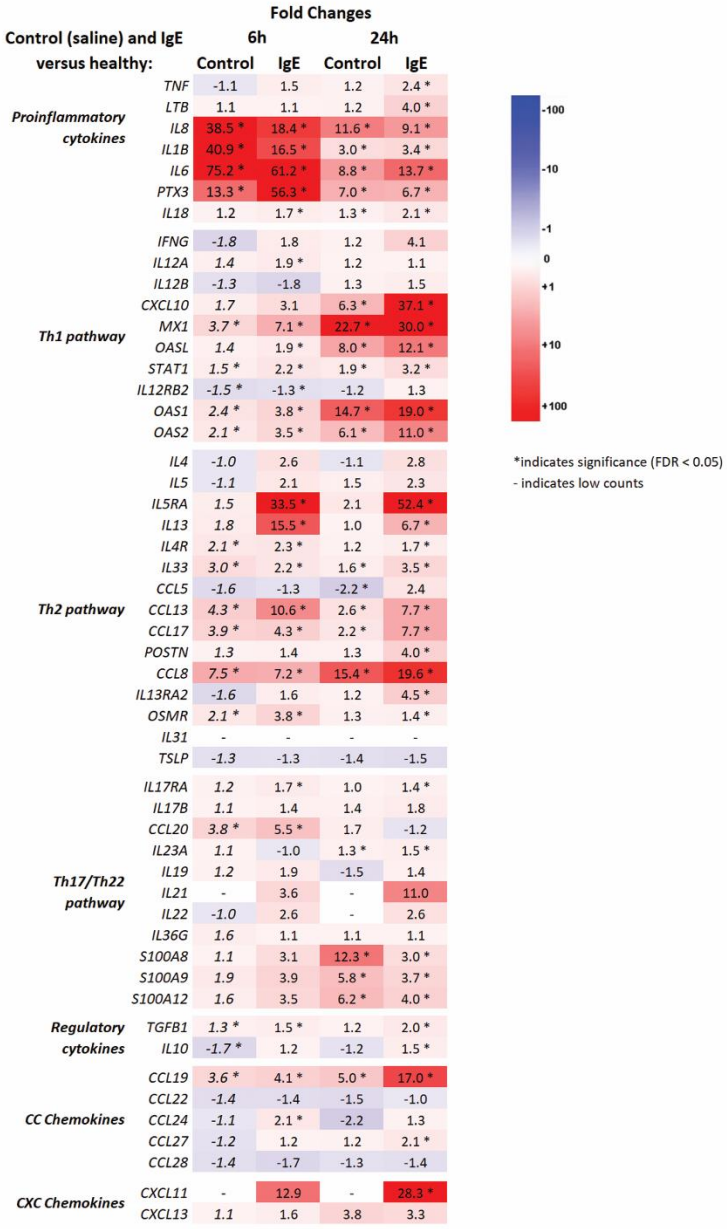

Figure 1.2. Expression of selected relevant cytokine, chemokine, and receptor genes in anti-canine-IgE and saline cutaneous reactions at 6 and 24 hr after intradermal injections. Gene are arranged by their dominant function or family and color responds to

downregulation (dark blue) and upregulation (bright red); bolded fold changes (FC) with asterisks are statistically significant at **false rate discovery (FDR)* < 0.05.

Anti-canine-IgE reactions showed stronger increase in Th2-related markers (e.g., IL-13, IL-4R, IL-5RA, CCL5, CCL13, CCL17, CCL24, POSTN, STAT6) compared to saline group; saline group did not reach significance for multiple Th2-related cytokines and chemokines (e.g., IL-13, IL-5RA, CCL24, POSTN, STAT6). In addition, there was an upregulation of IL-9R (FC = 7.9) only for anti-canine-IgE-mediated reaction at 24 hr; IL-9 (FC = 4.3) was upregulated as well, however, did not reach statistical significance (FDR = 0.05). Although significant modulation of several Th17/Th22-related markers (e.g., IL-17RA, IL-23A, CCL20, S100A12) was seen across both groups, there were no significant changes in key Th17 (i.e. IL-17A/IL-17F) and Th22 (i.e. IL-22) markers in both anti-canine-IgE and saline at 6 and 24-hr groups compared to healthy control.

We next evaluated genes associated with epidermal barrier differentiation and lipid synthesis (Guttman-Yassky et al., 2019; Sanyal et al., 2019)(Supplementary Table 1). While both interventions, the anti-canine IgE and saline injections, induced significant changes in epidermal barrier genes compared to healthy, only anti-canine IgE LPRs showed significant downregulation of terminal differentiation (FLG, FLG2, CDSN, LOR, LCE1E, LCE6A, CAPN1, ST14), gap/tight-junctions (CLDN1, CLDN4, CLDN5, GJB5) and lipid metabolism/biosynthesis markers (ELOVL1, ELOVL2, ELOVL6, ALOXE3). Saline and anti-IgE injections increased stress-associated (alarmin) keratins (KRT6A, KRT6B) and TIMP-1, a tissue inhibitor of metalloproteinase 1.

In the anti-canine IgE skin biopsy samples, several significantly up-regulated noncytokine pruritogens (Supplementary Figure S1.2) were genes encoding nerve growth factor (NGF) and its high affinity receptor NTRK1 (TrkA), the proteases cathepsin S (CTSS), chymase (CMA1) and the tryptic peptidase mastin, periostin (POSTN) and the enzymes involved in leukotriene-B4 (LTB4) synthesis (5-lipoxygenase [ALOX5] and its activating protein FLAP [ALOX5AP]) and the cysteinyl leukotriene receptor 1 CYSLTR1) and 2 (CYSLTR2) (Suppl. Table X). Both interventions (anti-canine IgE and saline injections) significantly upregulated the enzyme involved in histamine metabolism, histidine decarboxylase (HDC), and histamine receptor 1 (HRH1); however, only anti-canine IgE LPRs showed upregulation of histamine N-methyltransferase (HNMT at 24 hr) and histamine receptor 4 (HRH4 at 6 hr). Interestingly, anti-canine IgE injections significantly downregulated genes encoding substance P (TAC1), MAS-related GPR family member X2 (MRGPRX2) and endothelin

1 (EDN1). No significant differences in IL-31 expression existed between any interventions and healthy normal skin.

3.3. Pathway and enrichment analysis of anti-canine-IgE- and saline-mediated late phase reactions (LPRs)

To perform pathway-level comparisons across the molecular skin profiles induced by each agent, we conducted a Gene Set Variation Analysis (GSVA) using previously published immune gene-sets for Th1, Th2, Th17 and Th22_IL22 (Guttman-Yassky et al., 2019; Sanyal et al., 2019) (Figure 1.3).

Intradermal injection of saline induced elevated Th1 response at 24 hr; there was no significant increases in the Th1-, Th2-, Th17- and Th22-related pathways for any other time point. Anti-canine IgE injections showed significant upregulation in Th1-, Th2- and Th17-regulated genes at 6 and 24 hr; the Th22_IL-22 pathway was significantly elevated only at 24 hr.

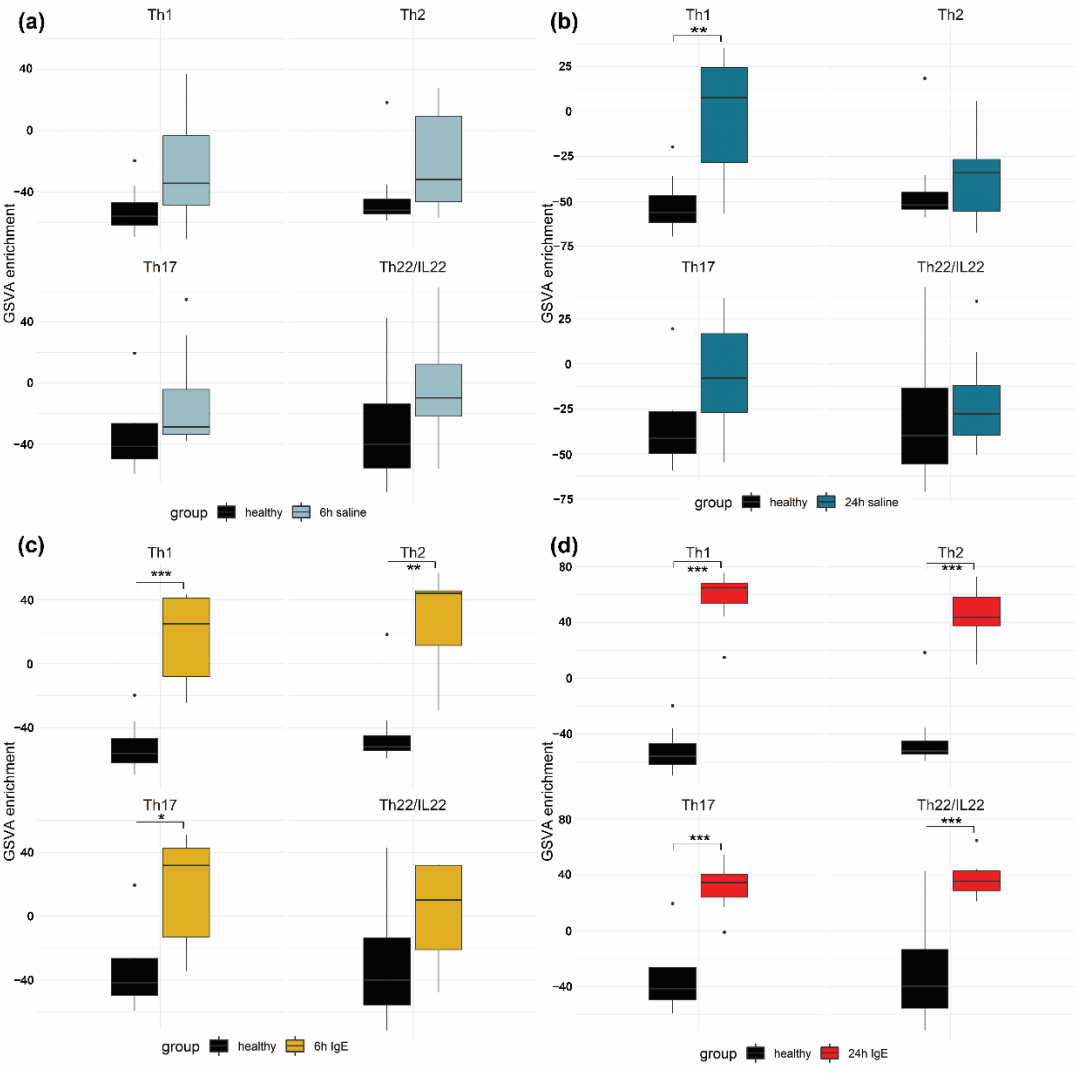

Figure 1.3. Gene Set Variation Analysis (GSVA) scores for T-helper (Th) 1, 2, 17 and 22/IL-22 immune pathway for each group (saline or anti-canine IgE) and time (6- or 24-hr) versus healthy demonstrated in vertical box and whisker plots. * implies *p-adj < 0.05, ** implies p-adj < 0.01, *** implies p-adj < 0.005. (a) 6-hr saline vs. healthy with no significance. (b) 24-hr saline vs. healthy with only Th1 showing significance. (c) 6-hr anti-canine-IgE vs. healthy with significance in Th1, Th2, and Th17 gene groups. (d) 24h-hr anti-canine IgE vs. healthy with significance in all GSVA gene groups.

To understand whether the DEGs are significantly enriched in the transcriptional enrichment and pathway analysis, upregulated and downregulated DEGs were analyzed by using Metacore software. Skin lesions induced by anti-canine-IgE injections at 6 and 24-hr induced 47 and 59 significantly upregulated process networks, respectively (Supplementary Table 1.2). In contrast, intradermal saline injections induced weaker responses at 6 and 24-hr with only 24 and 28 significantly upregulated process networks, respectively (Supplementary Table 1.2).

The top 20 most upregulated process networks (Supplementary Table 1.2) for anti-canine-IgE injections for both time points were related to the immune system, such as chemotaxis, JAK-STAT pathway, lymphocyte proliferation, leukocyte chemotaxis, interferon signaling, phagocytosis, antigen presentation, neutrophil activation, IL-4 signaling, NK cell cytotoxicity, T helper differentiation and innate inflammatory responses. There was also upregulation of inflammatory responses via IL-5-, IL-13- and IgE-signaling, histamine signaling and Th17 cytokine immune response.

The intradermal injections of saline control upregulated immune responses as well, such as chemotaxis, JAK-STAT pathway, cell-matrix interactions, extracellular remodeling, connective tissue degradation, phagocytosis, antigen presentation, neutrophil activation, innate inflammatory responses, Th17 cytokine immune response and IFN-y signaling. However, the number of upregulated genes in these pathways induced by saline control was significantly lower compared to anti-canine IgE-induced pathways. Furthermore, the robust immune response of interleukin signaling pathways associated with Th2 pathways, such as IL-4-, IL-5-, IL-13- and IgE signaling pathways,

which were increased in anti-canine-IgE reactions were not observed in saline control reactions at any time point.

Finally, the downregulated DEGs from anti-canine-IgE reactions at 6 and 24-hr induced 11 and 9 significantly downregulated process networks, respectively (Supplementary Table 1.2). The downregulated process networks were associated with neurogenesis synaptogenesis, neurogenesis axonal guidance, synaptic contact, transmission of nerve impulse, potassium and calcium transport, confirming the functional connection between the IgE activation of the immune system and free nerve endings in the skin. In contrast, there were only 2 and 4 significantly downregulated process networks from saline control DEGs at 6 and 24-hr, respectively (Supplementary Table 1.2); these networks were associated with translation initiation, muscle contraction, actin filaments and skeletal muscle development.

3.4. Quantitative real-time polymerase chain reaction (qRT-PCR)

Quantitative reverse-transcription PCR performed for selected genes (CCL2, C-X-C motif chemokine ligand 10 (CXCL10), CCL17, IL-1B, tissue necrosis factor alpha (TNF-α) and IL-33) at the 6-hr and 24-hr IgE timepoints were strong, at 0.90 ($p= 0.01$) and 0.93 ($p= 0.007$) correlation coefficients with a 95% confidence interval for Pearson correlations, respectively, demonstrating efficacy of RNA-seq to capture expression data accurately.

3.5. Correlation analysis to acute skin lesions in human and canine spontaneous AD

The search of the database identified only a single spontaneous human AD study that analyzed 38 healthy and 11 acute skin lesional AD samples using RNA seq at 125 base pairs; no spontaneous canine AD RNA seq studies that incorporated healthy and acute lesional AD skin samples using RNA seq analysis were found. Therefore, we investigated the overlap between these human orthologues of canine DEGs in anti-canine-IgE reactions at 6 and 24-hr and a previously published transcriptome skin data from acute spontaneous human AD skin lesions using criteria of -1.5 ≥ FC ≥ 1.5 and FDR<0.05. Spearman correlation coefficient for the shared DEGs between canine anti-canine-IgE and human AD samples revealed a significant moderate positive correlation for anti-canine-IgE 6-hr samples (1198 shared DEGs; r=0.53; P < 0.001; Figure 1.4a) and 24-hr samples (1020 shared DEGs; r= 0.47; P < 0.001; Figure 1.4b).

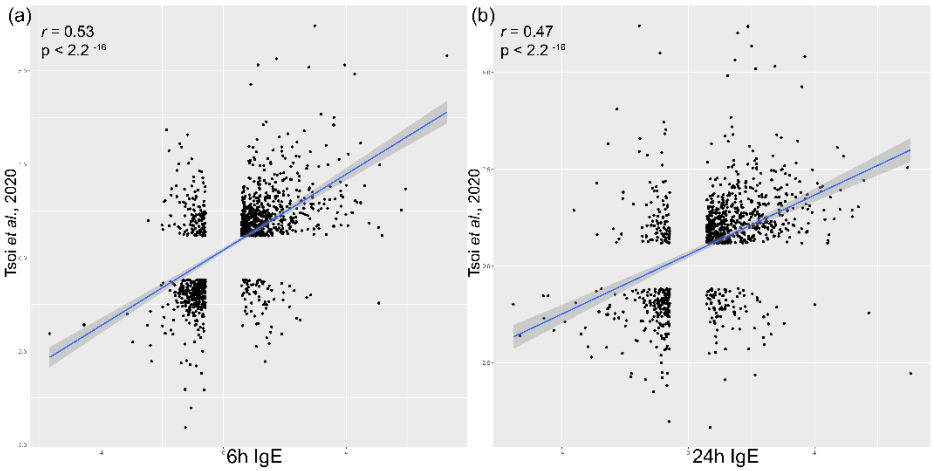

Figure 1.4. Spearman's rank test of differentially expressed genes (DEGs; -1.5 ≥ FC ≥ 1.5, FDR<0.05) between 6-(a) and 24-hr (b) anti-canine-IgE reactions and acute skin lesions of spontaneous human atopic dermatitis.

Discussion and Conclusions

This is the first global molecular profiling study of inflammatory skin lesions activated through IgE signaling in the skin of healthy dogs. Despite similar activation of pro-inflammatory genes in both groups, our data revealed significant variations in cellular infiltration and expression of immune and barrier genes between anti-canine-IgE and saline control skin lesions. With AD representing one the most prevalent inflammatory skin disease in humans and dogs, there is a need for the development of screening experimental models for studying the anti-inflammatory effect of anti-allergic drugs before entering clinical trials, like anti-canine-IgE reactions.

Historically, AD has been characterized as a biphasic disease with a Th2-to-Th1 transition from acute to chronic AD stage; however, there are conflicting data (Eyerich and Novak, 2013; Pucheu-Haston et al., 2015). To elucidate the transition from acute to chronic AD disease stages and the factors and mechanisms that shape chronic inflammatory activity, Tsoi et al. recently performed RNA sequencing on acute and chronic AD lesions within the same individuals (Tsoi et al., 2020). The results by Tsoi et al. in 2020 showed that the changes accompanying the transition from nonlesional to acute to chronic inflammation in AD are quantitative rather than qualitative; approximately 74% of the genes dysregulated in acute lesions remain or are further dysregulated in chronic lesions (Tsoi et al., 2020). All the major Th1, Th2, Th17 and Th22 responses were progressively heightened from nonlesional AD to acute and then chronic AD lesions, whereas nonlesional AD was enriched in Th2 and Th17 responses (Tsoi et al., 2020). In the study of this report, intradermal injections of anti-canine IgE in

healthy dogs induced acute multipolar Th polarization in the skin with early upregulation of Th1, Th2 and Th17 pathways at 6 hr and additionally at 24 hr for the Th22_IL-22 pathway. In addition, anti-canine IgE-mediated reactions transcriptomic profile was compared with the spontaneous acute human AD transcriptome to compare how well the IgE-induced skin lesions represent human AD. Previous studies utilizing murine AD-like models revealed that murine transcriptomes represent only 37%, 18%, 17%, and 11% of the human meta-analysis–derived atopic dermatitis profile (MADAD) for IL-23–injected, NC/Nga, oxazolone (OXA)-challenged, and ovalbumin (OVA)-challenged mice, respectively (Ewald et al., 2017). Interestingly, there were 1198 overlapped DEGs ($-1.5 \geq FC \geq 1.5$ and $FDR<0.05$) with moderate positive correlation ($r=0.53$) between the transcriptome of anti-canine IgE skin lesions at 6-hr and acute human AD in our study. Although IgE-induced lesions did not capture all immune and barrier aspects of chronic spontaneous human AD, the results of this study demonstrate that acute IgE-mediated signaling in skin induces a wide array of inflammatory axes, including Th2 activation, and could be suited in pre-clinical studies to evaluate Th2 AD-centric axis and how it communicates with other activated immune responses in AD patients.

Histologically, acute AD skin lesions in humans and dogs exhibit spongiosis with mild to moderate acanthosis in addition to a superficial perivascular infiltrate of lymphocytes, dendritic cells and macrophages (Leung et al., 1983; Olivry and Hill, 2001). In addition, mast cells can show degranulation, and occasionally eosinophils may be present with rare neutrophils (Leung et al., 1983; Olivry and Hill, 2001). Anti-canine IgE acute skin lesions in this study featured similar changes with mild acanthosis and superficial

dermis expanded by mild edema, intermixed with neutrophils, eosinophils, lymphocytes, and plasma cells; eosinophils and mononuclear cells dominated the late-phase reactions at 24 hr. Eosinophil recruitment to allergic inflammation sites in the skin and other tissues is driven by IL-5 signaling and by eotaxins (CCL11, CCL24, CCL26) and other chemokines such as regulated on activation, normal T cell expressed and secreted (RANTES; CCL5) and CCL3; these chemokines bind to eosinophils via the ß-chemokine receptor CCR3 (Matucci et al., 2019). The significant eosinophilic inflammation in the IgE-mediated skin lesions in this study compared to controls can be explained by the strong upregulation of IL-5 signaling pathway with IL-5RA (FC = 33.5 and FC= 52.4 at 6- and 24-hr reactions) as well as chemokines CCL3, CCL11 and chemokine receptor CCR3 (FC = 113.6 and FC= 79.5 at 6- and 24-hr reactions)

As previously mentioned, AD has long been considered a Th2 disease. A recent study revealed that IL13 is the dominant Th2 cytokine in spontaneous acute and chronic human AD skin lesions (Tsoi et al., 2019). Currently, IL-13 is considered the central driver of Th2 inflammation in human and canine atopic skin (Jassies-van der Lee et al., 2014; Tsoi et al., 2019). Interleukin 13, along with receptors IL4R and IL13Rα1, was the dominant Th2 cytokine in the anti-canine IgE skin lesions in this study, whereas IL-4 was not affected by the IgE-mediated activation. Interleukin 31 is another Th2 cytokine with a dominant pruritogenic effect across different species, such as humans, primates, mice, and dogs (Kunimura and Fukui, 2021; Pearson et al., 2023). Increased IL-31 serum levels have been observed in some AD dogs; a subset of dogs with AD had no detectable levels of IL31 in circulation (Gonzales et al., 2013). In this study, the RNA-

seq showed no significant upregulation of IL31 in any groups. Interestingly, previous murine and canine studies have also had issues amplifying IL31 in the skin of atopic dogs using RNA-seq (Arai et al., 2014; Tamamoto-Mochizuki and Olivry, 2021). It is possible that cutaneous IL-31 mRNA is temporary, unstable, and unpredictable or that the IL-31 sequence in the current canine genome utilized in RNA-seq analysis is not accurate and further studies using immunohistochemistry or immunofluorescence to target IL31 protein presence can be performed to elucidate the presence of IL31 in anti-canine IgE activated skin lesions.

Lesional AD skin features skin barrier dysfunction, characterized by multiple factors, including reduction of epidermal barrier proteins, ceramides, adhesion intercellular proteins and antimicrobial peptides (Guttman-Yassky et al., 2019; Sanyal et al., 2019; Tsoi et al., 2019). Th2 cytokines, IL-4 and IL-13, have been shown to downregulate the expression of skin barrier proteins and lipids in human keratinocyte cultures (Kubo et al., 2021). In contrast to saline control, anti-canine IgE-mediated inflammation significantly downregulated the expression of several epidermal proteins (FLG, FLG2, CDSN, LOR), tight-junction adhesion molecules (CLDN1, CLDN4, CLDN5) and lipid metabolism/biosynthesis markers (ELOVL1, ELOVL2, ELOVL6) in this study. The increased IL-13 expression with the lack of upregulation of IL-4 in anti-canine IgE skin lesions is likely the result of the observed skin barrier changes, resembling barrier dysfunction in spontaneous AD lesional skin in dogs and humans.

Some of the limitations in this study included a small sample size and a lack of identification of protein expression. We determined the sample size using the sample size calculator recommended for RNA-seq studies. In addition, the current canine protein multiplex assays have a limited number of markers available to analyze, in contrast to human assays that allow evaluations of up to 300 proteins (Mikhaylov et al., 2021). Furthermore, the batch effects present between samples in this study (specifically 75PE and 150PE reads depending on the sample) could cause a limit in the proper detection of DEGs by confounding the analysis. However, utilizing ComBat-seq, an extension of the ComBat approach, is optimal in this scenario as it works well on smaller sample sizes and is robust against outliers (Zhang et al., 2020).

In summary, the molecular characterization of experimental models utilized to evaluate therapeutics for spontaneous inflammatory skin diseases is essential for future mechanistic and immunomodulatory pre-clinical studies in humans and dogs. In this study, IgE-mediated skin lesions appear to mediate similar T-helper pathways and barrier changes to that of acute spontaneous human AD lesions through examination of the RNA-seq transcriptome; IL-13 represents the dominant Th2 cytokine in this model. Although the initial pilot study using qRT-PCR revealed that prednisolone reduced IL-13, IL-5, CCL2, CCL5 and CCL17 in IgE-mediated skin lesions, further molecular studies using RNA-seq should investigate the effect of established canine anti-allergic drugs (e.g., glucocorticoids, oclacitinib as JAK inhibitor) to validate the canine IgE model.

Supplementary Materials

The following supporting information below can be downloaded at: www.mdpi.com, Supplementary Material and Methods.

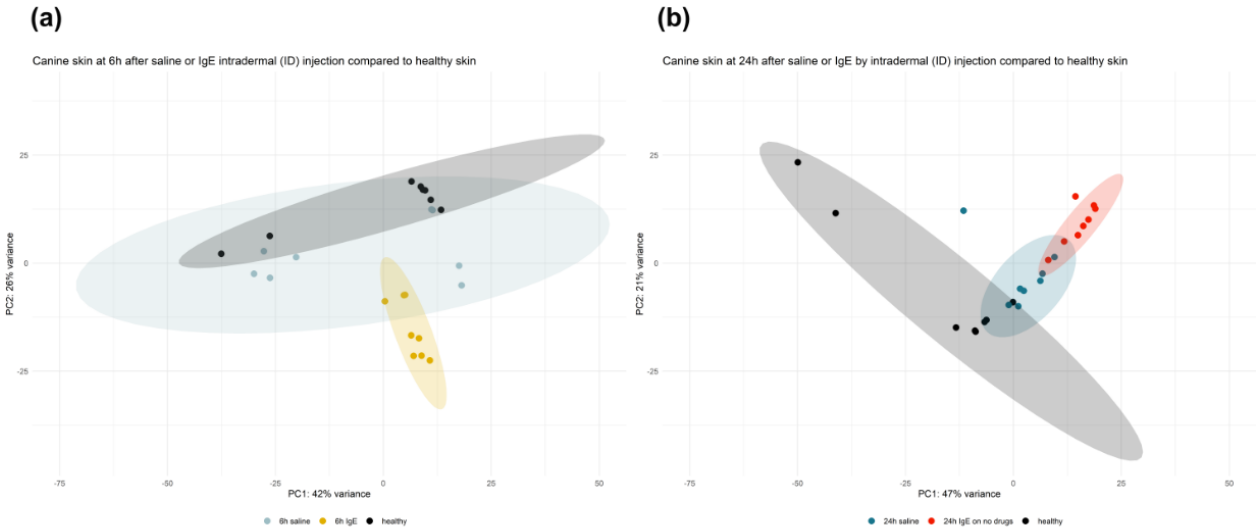

Figure S1.1: Principal Component Analysis (PCA) scores plot showing anti-canine-IgE and saline cutaneous reactions at 6 (a) and 24 (b) hr after intradermal injections.

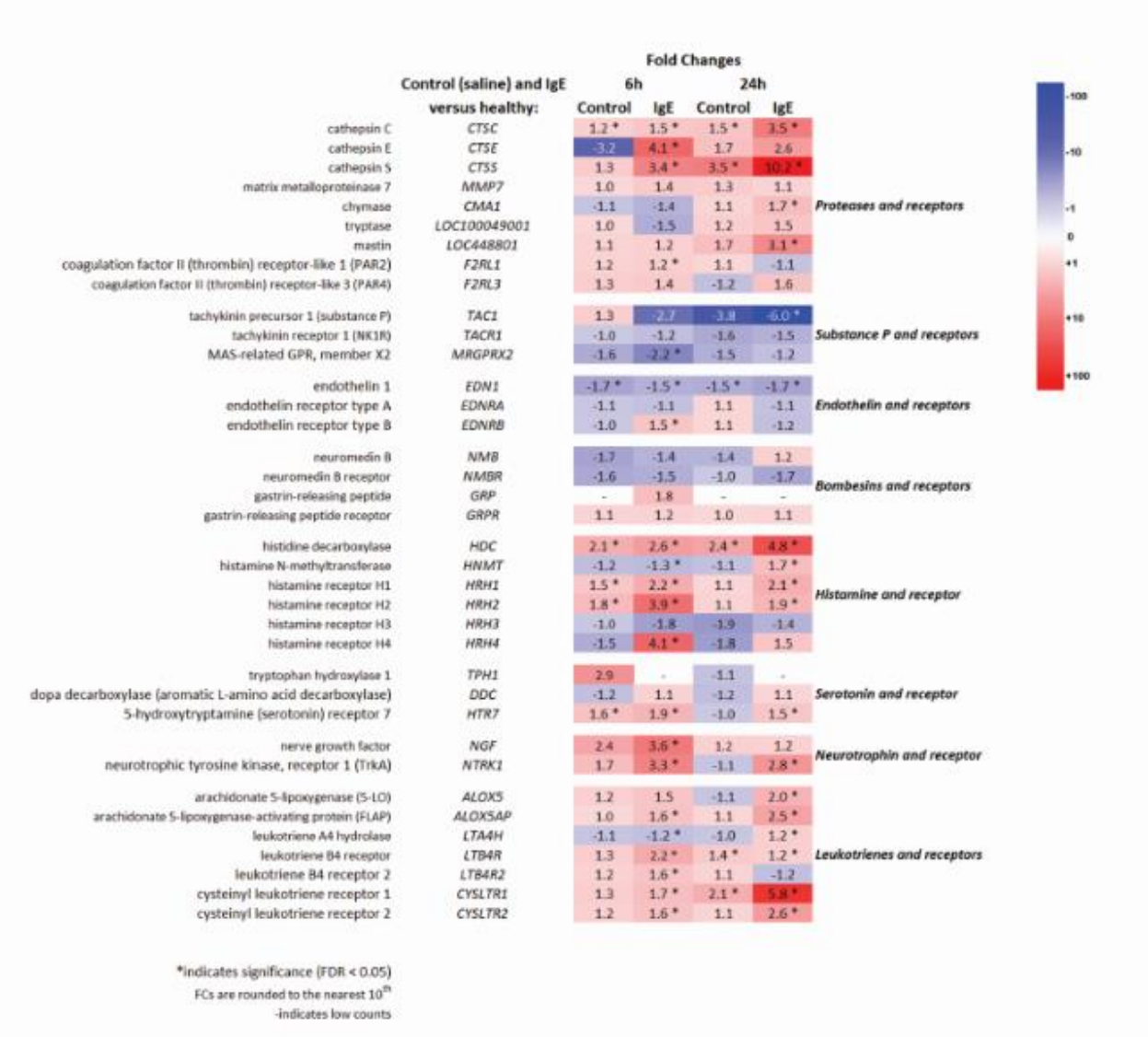

Figure S1.2: Expression of selected relevant pruritogens in anti-canine-IgE and saline cutaneous reactions at 6 and 24 hr after intradermal injections. Gene are arranged by their dominant function or family and color responds to downregulation (dark blue) and upregulation (bright red); bolded fold changes (FC) with asterisks are statistically significant at *false rate discovery (FDR) < 0.05.

Table S1.1: Statistically significantly differentially expressed genes (DEGs; false rate discovery (FDR) < 0.05) in anti-canine-IgE and saline cutaneous reactions at 6 and 24 hr after intradermal injections. Embedded excel sheets can be digitally explored.

gene_symbol	baseMean	log2FoldChange	UP or Down	Fold Change
TIMP1	4337.91572	3.829519632	UP	14.21674842
POLR1A	1368.84843	1.308411526	UP	2.476686952
WDR77	1001.38804	1.643128275	UP	3.123423672
NOC4L	1331.38217	2.192840748	UP	4.572048628
METTL1	513.012704	2.21862562	UP	4.654498137
GRWD1	438.486376	1.931007892	UP	3.813215041
PTX3	2820.60888	5.815737612	UP	56.32633167
BCAT1	822.411463	2.325123799	UP	5.011087742
SHQ1	605.333593	0.939226249	UP	1.917499563
LRRC59	3438.48888	2.189295357	UP	4.560826715
RRP12	1229.64049	1.436317953	UP	2.706292832
YARS	2492.63056	1.473609944	UP	2.777159321
FCGR1A	381.620611	4.690227932	UP	25.81661475
DKC1	2066.81834	1.701041898	UP	3.251356831
NARS	2847.59424	1.217896582	UP	2.326073336
SEMA3B	1008.77047	-1.412113276	Down	-2.661267028
FARSA	859.078813	1.413684934	UP	2.664167767

Table S1.2: Statistically significant Metacore process networks for upregulated and downregulated DEGs (Fold Change= +/- 1.5; false rate discovery (FDR <0.05) in anti-canine-IgE and saline cutaneous reactions at 6 and 24 hr after intradermal injections. Embedded excel sheets can be digitally explored.

Enrichment analysis report		
Enrichment by Process Networks		
#	Networks	Total
1	Chemotaxis	139
2	Inflammation_Jak-STAT Pathway	185
3	Proliferation_Lymphocyte proliferation	208
4	Cell adhesion_Leucocyte chemotaxis	180
5	Inflammation_Interferon signaling	110
6	Immune response_Phagocytosis	223
7	Apoptosis_Anti-apoptosis mediated by external signals vi	111
8	Inflammation_TREM1 signaling	145
9	Inflammation_Neutrophil activation	215
#	Inflammation_Amphoterin signaling	118

Author Contributions: Conceptualization, A.B. and F.B.; methodology, A.B. and F.B.; software, A.B. and F.B.; validation, A.B. and F.B.; formal analysis, A.B. and F.B.; investigation, A.B., K.H., S.J.K, J.E.F. and F.B.; resources, A.B., K.H., S.J.K, J.E.F. and F.B.; data curation, A.B. and F.B.; writing—original draft preparation, A.B. and F.B.; writing—review and editing, A.B., K.H., S.J.K, J.E.F. and F.B.; visualization, A.B., K.H., S.J.K, J.E.F. and F.B.; supervision, F.B.; project administration, A.B., K.H., S.J.K, J.E.F. and F.B.; funding acquisition, F.B. All authors have read and agreed to the published version of the manuscript.

Funding: This research was funded by Boehringer-Ingelheim Animal Health, grant number FP00012989.

Institutional Review Board Statement: The Institutional Review Board (or Ethics Committee) of the University of Georgia (protocol code A2016 08-017-Y3-A13) approved this animal study.

Data Availability Statement: Data is contained within the articles and supplementary material. The raw sequencing data is available upon request.

Acknowledgments: The authors would like to thank Tara Denley for the help in working with the dogs. Furthermore, we would like to thank Emma Guttman-Yassky and Ana Pavel for sharing the gene list for GSVA analysis.

Conflicts of Interest: The authors declare no conflict of interest.

Supplementary Material and Methods

Intradermal injections and skin biopsy collection of late phase reactions (LPRs)

The IgE-mediated LPRs model was performed as previously described (Pucheu-Haston et al., 2006). Dogs were sedated intravenously using medetomidine (Domitor, Pfizer, Exton, PA). After sedation intravenously using medetomidine (Domitor, Pfizer, Exton, PA) and local anesthesia, baseline healthy skin biopsies were obtained 7 days before the anti-IgE/control intradermal injections.

Around 48 hr prior to each injection, a large (about 10cm x 10cm) area for injection of the test substances was clipped on the right and left lateral thoracic region. This 48-hr delay prevented a skin reaction or irritation from clipping to interfere with the test. Dogs

were sedated intravenously using medetomidine for the testing and biopsy procedures. It has been established that medetomidine does not interfere with intradermal skin allergic testing reactions, including IgE-mediated LPRs, and histamine release in dogs (Banovic et al., 2020; Vogelnest, 2008).

Two intradermal injections of 0.05 mL of anticanine-IgE polyclonal antibodies (0.08 mg/mL, goat anti-canine IgE AHP946, Bio-Rad Laboratories, Inc., Hercules, CA, USA) and 0.05 mL phosphate-buffered saline (DILUENT, negative control; Sigma-Aldrich, St Louis, MO, USA) were administered on one side of the thorax and evaluated by an investigator (FB); histamine (0.1 mg/mL, Sigma-Aldrich) served as a positive control.

The order of injections was randomized for every dog using statistical computer software (GraphPad Prism 8.0) and the investigator (FB) was blinded during intradermal injection evaluations. The concentrations of the substances were chosen from the established intradermal-induced IgE-mediated cutaneous allergic reaction studies in dogs (Banovic et al., 2020; Olivry et al., 2001; Pucheu-Haston et al., 2006).

Clinical scoring involved a global wheal score (GWS) and LPRs. Twenty minutes after each injection, the extent and severity of the wheals were assessed by the same investigator (FB) who performed injections. Global wheal score was calculated from all measurements as previously reported: GWS = D × E × F (the average diameter (D) in orthogonal directions was measured in millimeters; erythema (E) and firmness (F). Six

and 24 hr following all intradermal injections, the global LPR score was determined as follows: LPR = E x I (erythema (E); the degree of skin induration (I)) (Pucheu-Haston et al., 2006).

Skin biopsy samples were collected from IgE-mediated cutaneous reactions at 6-and 24-hr post-injections; the 6- and 24-hr saline sample served a s negative control. All biopsies were bisected; one half was placed in neutral buffered formalin, and the other was immersed immediately in RNALater and kept frozen until RNA extraction.

Sample preparation for RNA sequencing

Total mRNA was extracted using miRNAeasy kit from Qiagen (Qiagen, Valencia, CA) following the manufacturer's specifications. Only samples with a 260/280 ratio of ~1.8-2.0 (RNA) and showing a ribosomal integrity number (RIN) above 7 were subjected to further library preparation and sequencing.

RNA sequencing data analysis

Forty RNA samples were analyzed in this study: eight healthy non-treated skin samples, eight samples from 6 and 24 hr post-intradermal saline (control) and eight samples from 6 and 24 hr post-intradermal anti-IgE injection. Sequencing was performed on NovaSeq 6000 with 150 paired-end base pairs (32 samples) and with the NextSeq 2000 with 75 paired-end base pairs (8 samples) according to the manufacturer's protocol (Illumina, San Diego, CA). Prior to analysis, data underwent batch effect adjustment for sequencing preparations using ComBat-seq; ComBat-seq is a batch effect adjustment

tool for bulk RNA-seq count data (Zhang et al., 2020). Coverage depth included an average of 23.3 million reads.

Data quality was assessed using FastQC (Andrews, 2010). Illumina standard primers were trimmed using Trimmomatic, additionally allowing a sliding window quality control and trimming of the data (Bolger et al., 2014). Paired-end reads were mapped to the canine (CanFam3.1) reference genome using TopHat2, keeping only uniquely concordantly mapped reads (Daehwan, 2013). Read counts per gene were accessed using HTSeq (Anders et al., 2015). In filtering counts, only genes with ≥ 1 read across samples were retained for further analysis.

Reverse transcription quantitative real-time PCR (RT-qPCR) analysis

To confirm the gene expression results from RNA seq data in this study, quantitative real-time PCR was performed for selected genes. Expression of CCL2, C-X-C motif chemokine ligand 10 (CXCL10), CCL17, IL-31 and interferon-gamma (IFN-y) was measured by quantitative reverse-transcription PCR (RT-qPCR). Total RNA was extracted from skin biopsy samples stored in RNALater solution using the RNeasy Mini Kit (Qiagen, Valencia, CA). The RNA quality was evaluated with an Agilent Bioanalyzer (Agilent Technologies, Santa Clara, CA, USA) and quantified by spectrophotometry. The average RNA integrity number for all samples was above 7, confirming high quality RNA for gene expression data. Skin RNA was reverse transcribed into complementary DNA (cDNA) by using the iScript cDNA Synthesis kit (Bio-Rad Laboratories, Hercules, CA, USA). The cDNA of selected genes using forward and reverse primers was amplified

with SYBR Green PCR Master Mix (Applied Biosystems, Foster City, CA, USA) in accordance with the instructions of the manufacturer. Primers were as follows (5′ to 3′): for CCL2, ACC TGC TGC TAT ACA CTC A (forward), TTG CTG CTG GTG ACT CTT (reverse); for CXL10, ACC TGT ATC AAG ATT AGT G (forward), GTC TTA GAT TCT GGA TTC A (reverse); for CCL17, CCA TCG TGT TTG TAA CTG T (forward), AAT ATC TGA CCG CCT TCT (reverse); for IL31, GAA ACC TTG CTG TCC TCC CA (forward), CCC CTG TCT CTT TCT TCT GAT AGT (reverse); for IFN-y, TTC TTC TGG CTG TAA CTG (forward), TTG GCT CTG AAT GAT TGT (reverse); and for HPRT, AGC TTG CTG GTG AAA AGG AC (forward), TTA TAG TCA AGG GCA TAT CC (reverse). All primers were validated, and agarose gel electrophoresis was used to confirm the correct size of the PCR product for all primer pairs. In addition, the PCR products for each primer pair were purified using QIAquick PCR Purification Kit (QIAGEN Inc., Valencia, CA, USA) and sequenced. The sequences were aligned using the ABI Sequencing analysis software, with contiguous sequences matched to the GenBank database using the Basic Local Alignment Search Tool (BLAST) to confirm that the expected transcript had been amplified (Zhang et al., 2000). The quantitative RT-PCR under the following conditions (3 minutes at 95 °C, then 40 cycles of 20 seconds at 95 °C, 1 minute at 55 °C, and 30 seconds at 72 °C) was performed in a CFX96 qRT-PCR machine (Bio-Rad Laboratories, Hercules, CA, USA). Cycle threshold (CT) values were standardized to the reference gene Hypoxanthine-guanine phosphoribosyltransferase (HPRT) and converted to fold change by using the $2^{-\Delta\Delta CT}$ formula (Livak and Schmittgen, 2001; Schlotter et al., 2009).

CHAPTER 4

TRANSCRIPTOME PROFILING OF SPONTANEOUS CANINE ATOPIC DERMATITIS LESIONAL AND NON-LESIONAL SKIN USING DEEP RNA SEQUENCING[2]

[2] Blubaugh, A; Goss, C; Denley, T; Guttman-Yassky, E; Pavel, AB; Banovic, F. To be submitted to *Allergy.*

Abstract

Background: Mouse models for atopic dermatitis (AD) are commonly used for preclinical research; these do not reproduce the complexity of human AD disease. Dogs naturally develop AD with similarities clinically and immunologically to their human counterpart. However, large scale transcriptomic studies evaluating global gene expression patterns and inflammatory pathways in canine AD have not been reported.

Methods: We characterized the atopic lesional (AL, 62 samples) and non-lesional (ANL, 29 samples) skin transcriptome in 33 AD dogs; 20 site-matching healthy skin samples from 12 dogs served as controls. Total RNA was extracted from skin biopsies and the transcriptome analysed using 150 paired-end RNA sequencing.

Results: The comparison of mRNA expression of spontaneous canine AL and ANL skin with healthy skin identified 5,259 and 1,711 differentially expressed genes (DEGs) at +/- 1.5-fold change (*P*-adjusted value <0.05) respectively. Top upregulated DEGs in AL and ANL skin were antimicrobial calcium-binding proteins *S100A12* and *S100A9*, keratinocyte gene *KRT2*, matrix metalloprotease *MMP12*, chemokines (*CCL5*, *CCL17*, *CCL22*, *CXCL10*) and interleukins (*IL*)-*8*, *IL-13*, *IL-26* and *IL-36G*; these genes expressed higher fold changes in AL skin in addition to significantly upregulated *IL-9*, *IL-17A*, *IL-17C*, *IL-22* and *IL-24*. Spearman correlation analysis utilizing a previously published human AD RNA-seq dataset revealed canine AL skin contained 6,475 shared DEGs (44%) with human AD (significant strong positive correlation rho=0.57, p < 2.2e-16).

Conclusion: Spontaneous canine AD skin exhibits a striking similarity to human AD skin with multipolar axis T helper cell gene markers and including Spearman correlation and offers a promising research alternative to mouse AD models.

Introduction

Mouse models for atopic dermatitis (AD) are commonly used for preclinical research, although these do not reproduce the complexity of the human disease. Dogs naturally develop AD with striking similarities both clinically and immunologically to their human counterpart. However, large scale transcriptomic studies evaluating global gene expression patterns and inflammatory pathways in canine AD have not been largely reported. We aimed to characterize the canine spontaneous atopic lesional (AL) and non-lesional (ANL) skin transcriptome of dogs using site-matching healthy (NN) skin. Our goals were to exemplify whether spontaneous canine AD holds biomolecular similarity to that of humans using raw sequencing data from a previously published human AD study (Tsoi et al. 2019) undergoing the same rigorous methodology, visualization, and quantitative measurable outcomes for direct comparison of the transcriptome.

Gene expression profiling of inflammatory skin diseases has been widely used to identify gene alterations in lesional and non-lesional skin compared to healthy skin to understand the molecular fingerprint, define pathogenic immune pathways, and identify disease-specific biomarkers for treatment. Initial transcriptome studies of visibly lesional and non-lesional AD skin utilizing microarray-based technology provided relevant insights into the skin barrier dysfunction and inflammatory changes of human (Esaki et al., 2015; Gittler et al., 2013; Gittler et al., 2012; Saaf et al., 2008; Suarez-Farinas et al., 2013a; Suarez-Farinas et al., 2011) and canine patients (Plager et al., 2012; Wood et al., 2009). However, the sample sizes were small and the microarray analysis has

limited coverage to detect all genes and low expressed transcripts (Tsoi et al., 2019). Recently, transcriptome studies based on RNA-sequencing (RNA-seq) have been instrumental to identify key transcripts and pathways in human AD skin lesions, establishing dominance of IL-13 pathways (Tsoi et al., 2019). The RNA-seq technique allows analysis of the entire genome compared to the limitations of microarray analysis. Unfortunately, the main limitation of these studies is the inability to evaluate the dynamics and fluctuations of the AD lesions, as one cannot precisely assess the age of biopsied skin lesions in canine or human patients with spontaneous AD.

Given that emerging AD treatments are designed to target specific inflammatory mediators or pruritogens, it is imperative to understand the molecular signature of spontaneous canine atopic dermatitis as a natural model of human atopic dermatitis. Our objectives were to characterize the activation of immunologic and pruritogenic pathways in spontaneous canine AD using RNA sequencing of skin biopsy samples obtained when no medications or injection treatments of AD were being utilized. Furthermore, we performed a comparative analysis of the differentially expressed genes (DEGs) and transcriptional pathways unique to spontaneous canine AD and recently published RNA-seq transcriptome data of human AD skin biopsies via Spearman correlation coefficients.

Materials and Methods

2.1 Dogs

62 lesional (AL) and 29 non-lesional (ANL) samples from 33 canine spontaneous atopic dermatitis dogs were collected. 20 site-matched (axillae region to axillae region, e.g.) healthy (NN) skin samples from 12 healthy dogs were collected. The dogs ranged in age from 1-12 years old. A variety of 16 different breeds were used (German Shepherd Dog, Dachshund, Golden Retriever, Mixed breed, e.g.).

2.2 Clinical Study

2.2.1 Skin Sample Collections

Human raw sequence data and corresponding metadata were obtained from Tsoi et al. 2019 available through NCBI GEO accession GSE 121212 using SRA-Toolkit. Raw sequence reads were accessed for quality and trimmed using the same programs as mentioned below for canine samples, as were alignment, sorting, and gene count obtainment with the same stringencies; sequences were aligned to the GRCh38 reference genome annotation release 106. For canine sample collection, owners provided consent (written and verbal) prior to the procedure. Inclusion criterion involved a CADESI-04 (Canine Atopic Dermatitis Extent and Severity Index) score ≥ 35 with no history of medications within their washout period (e.g., cyclosporin, glucocorticoids) (Figure 2.1). Lesional and non-lesional samples were collected at least 7cm away from each other to ensure representative samples (Figure 2.2).

Figure 2.1. Canine AD skin sampling examples of presenting patients in the study. Note the erythema and lichenification of the skin.

Figure 2.2. Biopsy sampling sites; non-lesional (left) and lesional (right). Sites matched in location to healthy canine skin samples.

2.2.2 RNA Sequencing

RNA was isolated using the Qiagen RNeasy kit. A RIN (RNA Integrity Number) of > 7 (on a scale of 1-10) was used for quality control (QC) prior to sequencing. 150 PE (paired-end) sequencing was done using the Novaseq 6000; poly-A enrichment was used for mRNA. Sequences were aligned to the CanFam3.1 reference genome using TopHat2 after QC using FastQC and trimming with Trimmomatic. Gene counts were obtained from sequence alignment using Samsort and HTSeq.

2.2.3 Correlation to Human AD

Human raw sequence data and corresponding metadata were obtained from Tsoi *et al*. 2019 available through the NCBI GEO accession GSE121212 using SRA-Toolkit. Raw sequence reads were accessed for quality and trimmed using the same programs as mentioned above for canine raw reads, as were alignment, sorting, and gene count obtainment with the same stringencies; sequences were aligned to the GRCh38 reference genome annotation release 106. Spearman correlations were performed during subsequent R analysis (below).

2.2.4 Principal Component Analysis (PCA), Differential Expression (DE), and Gene Set Variation Analysis (GSVA)

Subsequent PCA, DE, GSVA, and correlation visualization and analysis were performed using R (ver. 4.04) with packages ggplot2, DESeq2, and GSVA. Differentially Expressed Genes (DEGs) in DE were defined as having a False Discovery Rate (FDR) < 0.05 and a Fold Change (FC) ≥ 1.5 or ≤ -1.5.

Correlation between significantly upregulated/downregulated DEGs (FC= +/- 1.5; FDR<0.05) of spontaneous reactions at 6- and 24-hr and spontaneous human and canine AD lesional skin specimens was evaluated using Spearman correlation coefficients on log2-transformed levels as previously described. Data were presented in scatterplots with estimated linear regression and a 95% confidence interval.

Normalization of RNA-seq data and DE analysis between different conditions (e.g., healthy, atopic non-lesional, atopic lesional) was performed using empirical Bayes linear model, DESeq2, as implemented through the vignette (Love et al., 2014). A false discovery rate (FDR) of less than 0.05 and fold change (FC) of +/- 1.5 or greater was used to determine differentially expressed genes (DEGs). Phenotypically unbiased evaluation of gene set variation between groups was performed with Gene Set Variation Analysis (GSVA) (Hanzelmann, 2015; Ritchie et al., 2015). Functional enrichment analysis for pathway identification was done using the Metacore platform for all DEGs (Freudenberg et al., 2019; Metacore, 2023).

Results

3.1 Principal Component Analysis

Principal component analysis showed a transcriptomic separation of AL and ANL from the NN skin's molecular fingerprint; the separation is more pronounced for AL samples than for ANL samples, as has been observed in human AD (Figure 2.3).

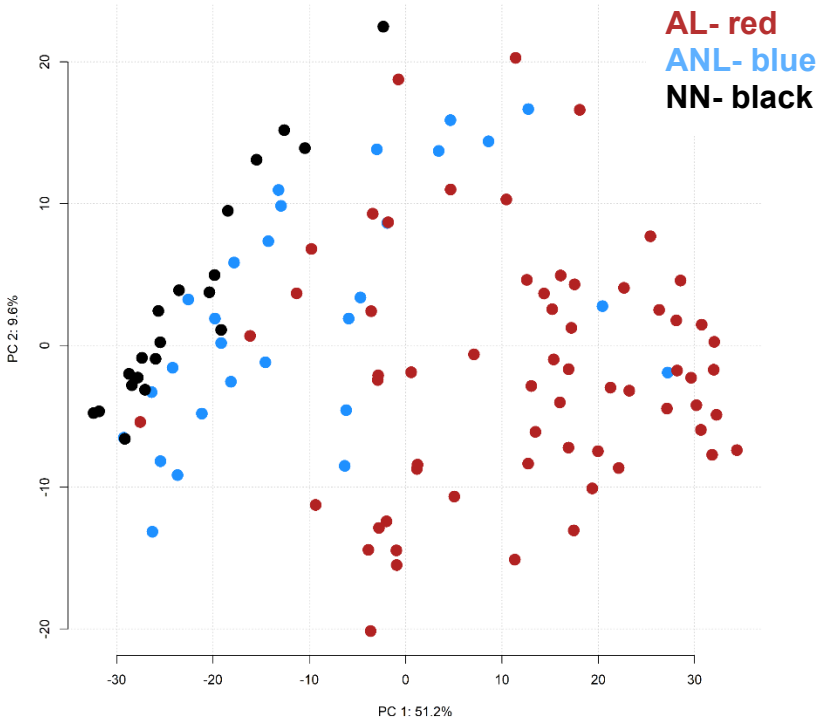

Figure 2.3**.** Spontaneous Canine cAD and Healthy Principal Component Analysis (PCA) The molecular dispersion of ANL and AL skin to that of NN skin, as seen in canines here, was similar to dispersion of human samples in Tsoi *et al*.

3.2 Differential Expression

Top upregulated DEGs in AL and ANL skin were antimicrobial calcium-binding proteins S100A12 and S100A9, keratinocyte gene KRT2, matrix metalloprotease MMP12, chemokines (CCL5, CCL17, CCL22, CXCL10), and interleukins (IL)-8, IL-13, IL-26, and IL-36G. These genes expressed higher fold changes in AL skin, in addition to significantly upregulated IL-9, IL-17A, IL-17C, IL-22, and IL-24 (Figure 2.4).

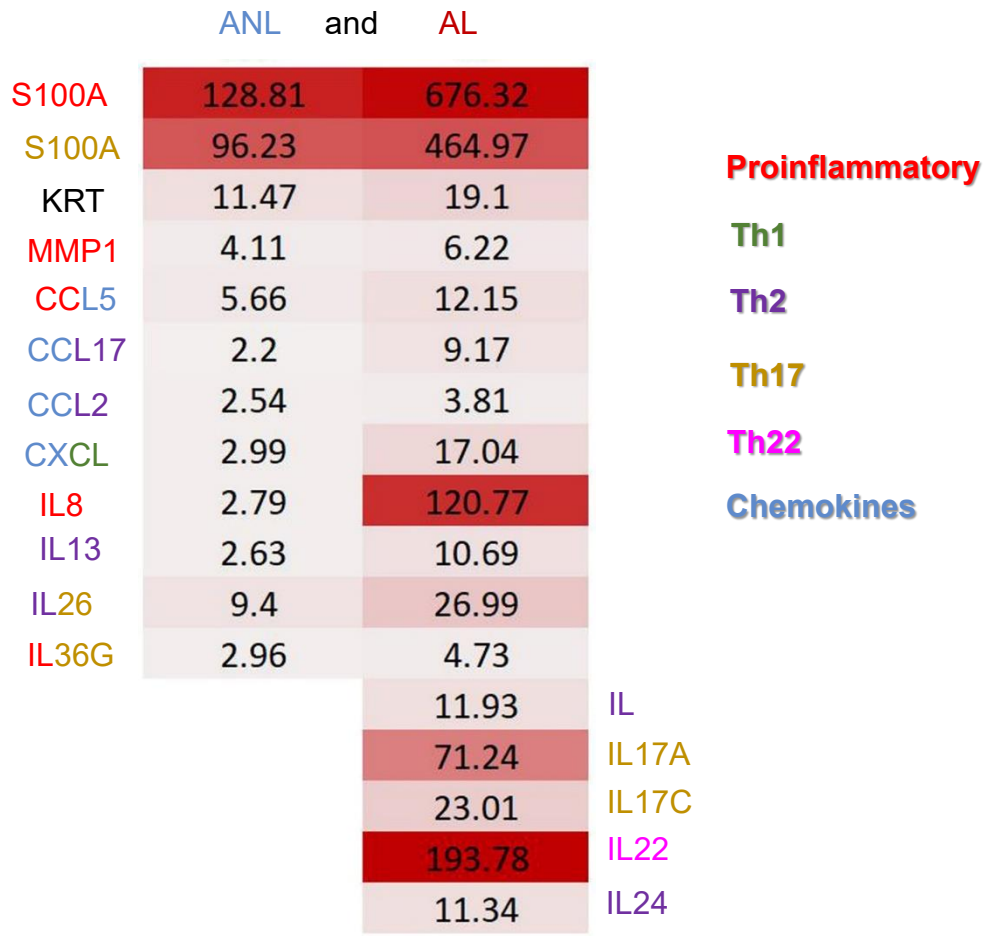

Figure 2.4**.** Heatmap of DEGs of interest and their respective FCs in canine ANL and AL skin. DEGs are highlighted by color (key to the right of the heatmap), represented by their respective immunological role(s) when possible. Of note is the IL-13 dominance among Th2 cytokines in ANL and AL skin, as has been shown in human AD.

3.3 Gene Set Variation Analysis

Phenotypically unbiased analysis of T-helper (Th) gene sets was performed, with genes used to represent each T cell helper (Th) group shown below. This revealed significant upregulation of all multipolar immunological axes in ANL skin with more robust Th2,

Th22, and Th17 responses. All the major Th responses progressively heightened in AL skin; mirroring changes observed in human AD (Figure 2.5).

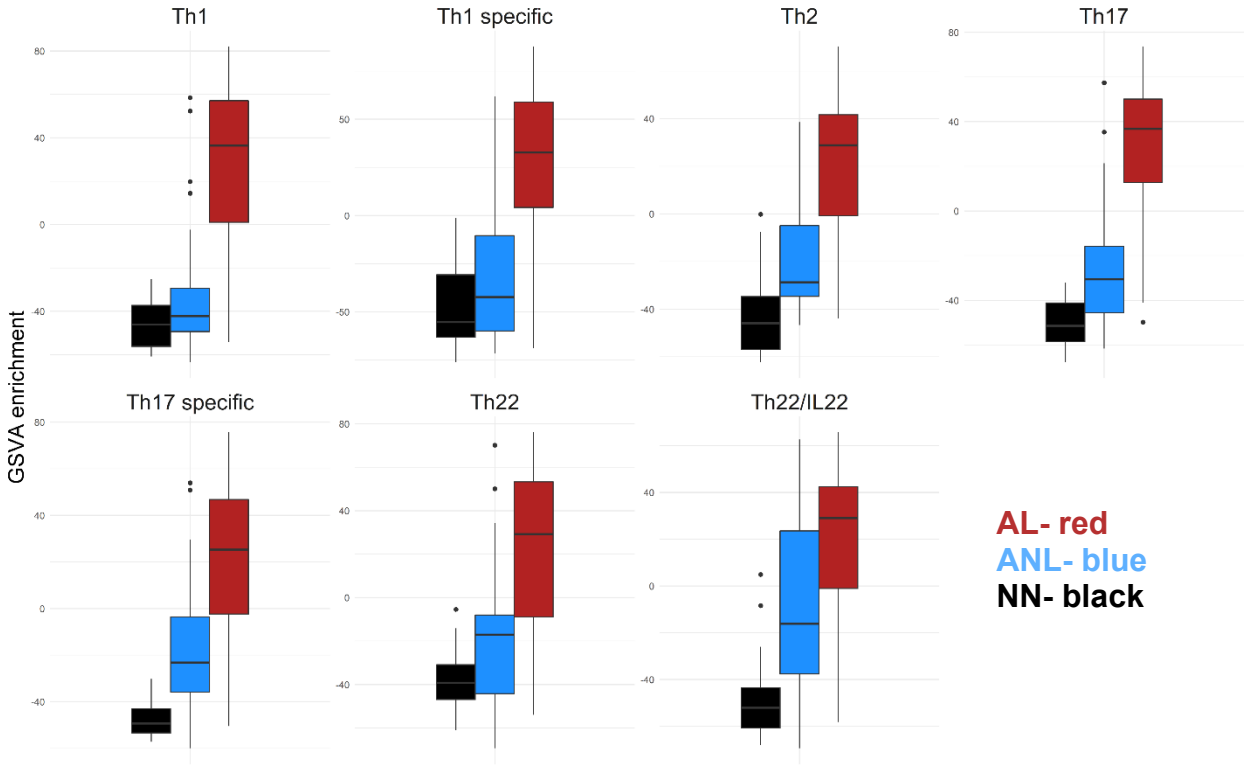

Figure 2.5**.** GSVA of immunological axes in healthy and spontaneous cAD. GSVA enrichment scores by group (NN, ANL, and AL) are graphed for each Th group. Significant upregulation of all multipolar immunological axes in ANL from NN skin were present, with more robust Th2, Th22, and Th17 responses. All major Th responses progressively heightened from NN to NL and with further significance in AL from ANL and NN skin; mirroring changes observed in human AD.

3.4 Spearman Correlation

Spearman correlation revealed a strong positive correlation (rho (ρ)= 0.57) between DEGs of canines and humans (Figure 2.6), with just over 44% of all Tsoi AL DEGs shared with canine spontaneous AL DEGs (Figure 2.7).

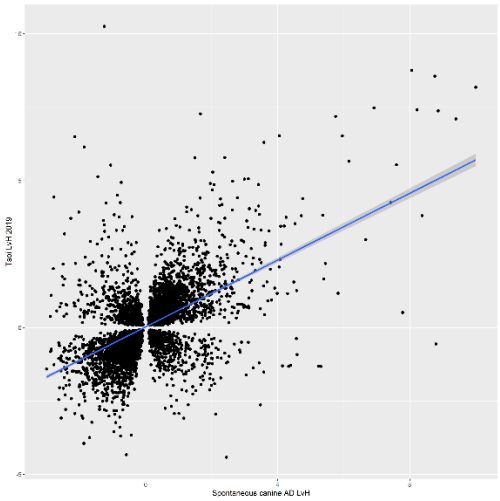

Figure 2.6**.** Spearman Correlation of DEGs from each study (Tsoi 2019 human AD and spontaneous cAD). Spearman correlation ($p < 2.2e-16$, S= 2.2e10, rho (ρ) < 2.2e-16 at a 0.95 confidence interval (CI)) showing all shared DEGs (FDR < 0.05) by FC in spontaneous canine AD AL v NN (x-axis) and FC in spontaneous human AD AL v NN (y-axis). The graphic line represents the best generalized linear model (glm) between the corresponding FCs.

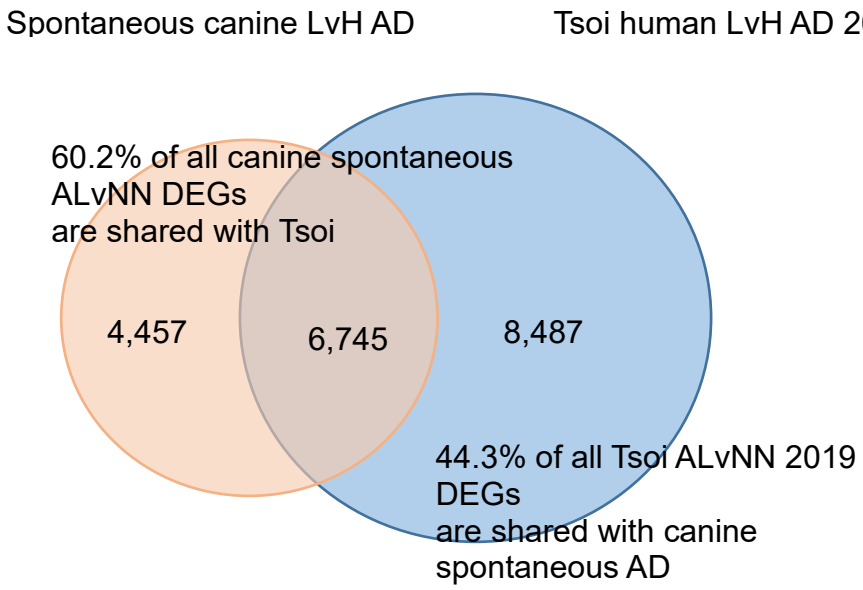

Figure 2.7. Venn diagram allowing visualization of the overlap in common DEGs (Tsoi 2019 human AD and spontaneous cAD). (FDR < 0.05) shown by raw gene number and percent between AL v NN in spontaneous canine AD and human AD.

Discussion and Conclusions

This is the first global molecular profiling study of lesional and non-lesional skin in canine spontaneous AD using deep RNA sequencing.

Recent molecular phenotyping studies in chronic AD skin lesions of pediatric, European/American AD, and Asian AD populations have shown significant variability in Th-axis (Th1, Th2, Th17, Th22) involvement and epidermal barrier characteristics (Roduit et al., 2017; Sanyal et al., 2019). However, a strong Th2-axis up-regulation has been consistently observed across all AD populations. The observed variability in these studies is likely the consequence of the different chronic disease stages of AD among

populations. Historically, AD has been characterized as a biphasic disease with a Th2-to-Th1 transition from acute to chronic AD stage; however, there are conflicting data (Grobe et al., 2019). Tsoi et al. recently performed RNA sequencing on acute and chronic AD lesions within the same individuals to elucidate the transition from acute to chronic AD disease stages and the factors and mechanisms that shape chronic inflammatory activity. The results by Tsoi et al. showed that the changes accompanying the transition from nonlesional to acute to chronic inflammation in AD are quantitative rather than qualitative; approximately 74% of the genes dysregulated in acute lesions remain or are further dysregulated in chronic lesions. All the major Th1, Th2, and Th17 responses were progressively heightened from nonlesional AD to acute and then chronic AD lesions, whereas nonlesional AD was enriched in Th2 and Th17 responses. The Th22 response, mediated by the dominant cytokine IL-22 responsible for epidermal hyperplasia in chronic AD skin lesions, was upregulated in both acute and chronic AD lesions.

In this study, we showed that non-lesional skin of spontaneous canine AD contains significant upregulation of all multipolar immunological axes with more robust Th2, Th22, and Th17 responses. However, all the major Th responses progressively heightened in canine AL skin, mirroring changes observed in human AD. Previous studies utilizing murine AD-like models revealed that murine transcriptomes represent only 37%, 18%, 17%, and 11% of the human meta-analysis–derived atopic dermatitis profile for IL-23–injected, NC/Nga, oxazolone (OXA)-challenged, and ovalbumin (OVA)-challenged mice, respectively (Ewald et al., 2015). In our study, there was around 44% overlap in DEGs with a good positive correlation between lesional canine AD and

human AD, which is more than murine AD-like models. The results of this study confirm that spontaneous canine AD lesional skin displays a robust molecular resemblance to human AD skin.

As previously mentioned, AD has a long time been considered a Th2 disease. A recent study revealed that IL13 is the dominant Th2 cytokine in spontaneous acute and chronic human AD skin lesions (Tsoi et al., 2019). This was a surprising finding as AD has, for a long time, been considered a Th2 disease with predominant IL4 cytokine responses. The half-life of the interleukin 4 *in vivo* is short and shares much of its biology with the IL13 cytokine, while the heterodimeric receptor IL4R/IL13Rα of IL13 is shared with IL4. Interleukin 13, along with receptors IL4R and IL13Rα1, was the dominant Th2 cytokine in the non-lesional and lesional canine AD skin in this study, whereas IL-4 did not show any changes in the skin.

In conclusion, spontaneous canine AD skin displays molecular resemblance to human atopic dermatitis, as immunological axis upregulation of spontaneous canine AD is also similar in human spontaneous AD. Canine AD offers a promising preclinical research alternative to mouse AD models. Many genes in the canine genome share homology with humans, making translational medicine directly relevant. Further, the FDA only recently approved several JAK inhibitors for treatment of human AD; JAK inhibitors such as oral oclacitinib (Apoquel, Zoetis, USA) have been in use since 2013 for dogs with AD. It is not unfounded that future canine AD studies yielding novel therapies would be relevant to the potential understanding and treatment of human AD.

Author Contributions

Conceptualization, A.B. and F.B.; methodology, A.B., F.B., A.B.P., E.G.Y.; software, A.B. and F.B.; validation, A.B. and F.B.; formal analysis, A.B. and F.B.; investigation, A.B., F.B., A.B.P., E.G.Y.; resources, A.B., C.G, T.D. and F.B.; data curation, A.B. and F.B.; writing—original draft preparation, A.B. and F.B.; writing—review and editing, A.B., F.B.; visualization, A.B., E.G.Y. and F.B.; supervision, F.B.; project administration, A.B. and F.B.; funding acquisition, F.B. All authors have read and agreed to the published version of the manuscript.

Acknowledgements

The authors would like to thank all clients who consented to enroll their dogs in this study, as well as the research institute at Mount Sinai for providing curated gene lists for GSVA.

Funding Information

This study was partially funded by the American Kennel Club (AKC).

Conflict of Interest Statement

None declared.

Data Availability Statement

Data is contained within the article. The raw sequencing data is available upon request.

ORCID

Amanda L. Blubaugh https://orcid.org/0000-0002-3918-6004

Frane Banovic https://orcid.org/0000-0002-4785-4121

Emma Guttman-Yassky https://orcid.org/0000-0002-9363-324X

Ana Brandusa Pavel https://orcid.org/0000-0002-0497-8351

CHAPTER 5

CHARACTERIZATION OF A CHLOROQUINE-INDUCED CANINE MODEL OF PRURITUS AND SKIN INFLAMMATION[3]

[3] Blubaugh, A; Denley, T; Banovic, F. 2020. *Veterinary Dermatology*. 31(2), 128-133. https://doi.org/10.1111/vde.12818.

Reprinted here with permission of the publisher.

Abstract

Background: Chloroquine (CQ) is a prototypical systemic and intradermal pruritogen for histamine-independent (nonhistaminergic) itch in mice and humans. The predictive validity of this model is poorly documented in dogs.

Hypothesis/Objective – To determine pruritogenic and inflammatory effects of systemic and i.d. CQ injections in healthy dogs.

Animals – Ten healthy purpose-bred laboratory beagles.

Methods and materials – All dogs were randomized to receive i.d. (200 and 400 μg/site), intravenous (2 mg/kg) and subcutaneous (3 mg/kg) CQ injections. Dogs were video recorded for 30 min after i.d. injections and for 300 min after i.v. and s.c. injections. Buffered saline injections served as controls for each route. Global wheal scores were evaluated at 30 min post-i.d. injection by a blinded investigator.

Results – All dogs showed wheal and erythema at the CQ i.d. injection sites; global wheal scores of each CQ concentration were significantly increased compared to placebo ($P \leq 0.05$). Blinded evaluation revealed no significant increase in generalized pruritic behavior (pruritic seconds) after i.v. or s.c. administration of CQ. Intradermal injections induced mild localized acute pruritic behaviors at the site of injections at 200 μg ($P = 0.06$) and 400 μg ($P = 0.27$) CQ in dogs.

Conclusion and clinical significance – To the best of the authors' knowledge, this is the first report which shows that i.d. CQ injections may induce acute inflammation in healthy dogs. By contrast to the systemic CQ-induced pruritus reported previously in healthy mice and dogs, no significant pruritic behaviors were observed after CQ injection, regardless of the route of administration.

Introduction

Pruritus (itch), defined as a sensation that provokes a desire to scratch, is the most common symptom of many dermatological diseases in dogs (Hensel et al., 2015). Basic research has advanced our understanding of the mechanisms underlying pruritus. In healthy humans and mice, histamine-dependent and histamine-independent (non-histaminergic) pathways have been identified to mediate acute and chronic itch sensations (Akiyama et al., 2010; Yosipovitch et al., 2018).Since histamine is not a potent acute itch inducer in dogs (Banovic et al., 2019) and first-generation antihistamines have shown limited efficacy in control of canine pruritus (Olivry et al., 2015), there is a need to investigate the non-histaminergic itch pathways in dogs for the potential development of novel drugs to block itch pathways.

Chloroquine (CQ) is a drug that has long been used in the treatment and prevention of malaria. A significant side effect of CQ in some humans is itch that cannot be ameliorated by systemic antihistamines (Abila et al., 1994; Ajayi, 1989; Tarrasón, 2017). Systemic and intradermal CQ injections into healthy mice induce itch that is transduced via Mas-related G protein-coupled (Mrgp) receptors (Foroutan et al., 2015; Liu et al., 2009; Tarrasón, 2017). Therefore, CQ is considered a prototypical systemic and intradermal pruritogen for histamine-independent itch in mice and humans (Liu et al., 2009; Tarrasón, 2017). In a recent study, systemic CQ administration induced pruritus in healthy beagles (Aberg et al., 2015), however, the predictive validity of this model is poorly documented in dogs.

The objectives of this study were to characterize systemic and intradermal CQ provoked itch behaviors and global wheal scores in healthy canine skin with a goal of developing a canine model for non-histaminergic itch.

Materials and Methods

Study population

Ten clinically healthy male castrated research beagle dogs with no previous history of pruritus or skin disease were included in this study. The dogs ranged in age between 1 to 2 years and were housed in a university setting under standard conditions. The dogs had not received any medications for at least 12 weeks prior to enrolment. All aspects of the study were approved and conducted in accordance with the Institutional Animal Care and Use Committee (IACUC).

Study protocol

The study was designed as a crossover study where every dog serves its own control. This number of dogs was deemed sufficient for this study to have a 90% power to detect a significant two-fold difference in values (pruritic scores) between controls and CQ administration (SD of 30% at P = 0.05; 1 sided: post < before; http://powerandsamplesize.com/Calculators/). All dogs were examined by the investigators and confirmed healthy and free of any dermatological or systemic disease five days prior to the first study day.

Interventions

Chloroquine (Sigma/Aldrich, St. Louis, MO, USA) was purchased and dissolved in sterile buffered saline (Sigma/Aldrich) for the systemic administration to a concentration of 20 mg/mL; sterile phosphate buffered saline served as a negative control for all experiments.

This study was divided into three phases: intravenous (IV), subcutaneous (SC) and intradermal CQ administration. All dogs received IV CQ at 2 mg/kg (slowly over 2-3 min) and saline injections at two independent occasions (total of 4 IV interventions). Subcutaneous CQ at 3 mg/kg and saline were injected on the thorax between the shoulder blades. The evaluated CQ dosages were selected from the previous study evaluating CQ-induced itch in dogs (Aberg et al., 2015). Localized pruritus was evaluated after intradermal chloroquine injections at 200 and 400 µg/site; two buffered saline injections served as control (total of 4 intradermal interventions). The CQ intradermal dosages were chosen from the established CQ-induced itch studies in murine models (Foroutan et al., 2015).

Randomization

The treatment groups for dogs for IV, SC and intradermal CQ administration were randomly divided using statistical computer software (Prism 8.0; GraphPad Softwares, La Jolla, CA, USA). Both clinical investigator and the video evaluators were blinded to the group assignments. The randomization sequence was unmasked only at the end of the study. There was a 3-week wash-out between different phases (IV, SC and intradermal).

In the first phase, the dogs were randomized and administered CQ or saline through IV injections with at least 14 days washout between IV injections (Aderounmu and Fleckenstein, 1983). During the second phase, dogs were randomly assigned to receive SC CQ or saline with a 14-day washout between the SC injections. The washout period was selected based on the previous CQ study in dogs (Aberg et al., 2015).

After 21 days washout from the last SC CQ administration, intradermal CQ phase was initiated. A small (about 7cm x 7cm) area for CQ intradermal injection was clipped on the right and left lateral thoracic region; all injection site clippings were performed at least 48 hr prior to each injection in order to avoid any occurrence of localized skin reaction or irritation in concurrence with the administration and evaluation of the CQ/saline. Chloroquine at 200 and 400 µg/site was intradermally injected with two separate rounds of intradermal buffered saline as a negative control (Liu et al., 2009). To avoid residual inflammation from the previous injection, injections were rotated to alternate side between the left and right sides of the thorax with a washout period of 3 days (Banovic et al., 2019).

Video recordings

Dogs were acclimated to their kennels and recording video equipment for at least one week prior to recording. All dogs were video recorded using GoPro Hero Session (GoPro, Inc., San Mateo, CA, USA) high-definition, waterproof cameras; the cameras were placed in the kennels to assure that each dog was fully visible for the duration of

the recording period. All injections, as well as the video recordings, were performed at the same time of the day without the investigators presence during the filming. All dogs were single housed in their kennels during the study. All toys were removed immediately before recording and only food and water were available at the time of injections. For the SC and IV phase itch evaluations, the video recordings were completed for a total of consecutive 300 minutes (5 hr) post-injections. For the intradermal CQ/saline acute itch evaluations, video recordings were evaluated for the 30 minutes after injections. The duration of CQ/saline video recordings resembled previously published CQ-induced itch study in dogs (Aberg et al., 2015) and mice (Foroutan et al., 2015).

Assessment of pruritus

A canine ethogram for itch behavior was drafted from previous studies in dogs (Table S1) (Banovic et al., 2019). Systemic and localized pruritic behavior measurements in areas of intradermal injections were completed using the ethogram. Behaviors were defined in the written definition and with video example for observers to objectively quantify the presence of pruritic behavior. Behaviors quantified included licking, biting/chewing, scratching, head shaking, scooting, rolling, pawing, and rubbing, whereas flinching from the site of injection or vocalization was considered to be indicative of pain (Banovic et al., 2019; Carr et al., 2009). Two trained investigators divided and reviewed the video recordings. First, the interobserver reliability for the pruritic behaviors was blindly evaluated by the two investigators on the video recordings from 10 dogs. There was a highly significant correlation between pruritic seconds obtained by both investigators for the identical videos (Spearman's $r= 0.94$; $P < 0.001$).

This correlation was a marker of satisfactory interobserver reliability for further study evaluations.

The video recordings in this study were coded, randomized and the investigators were blinded to the route of administration as well as substances administered until all data were analyzed. Investigators evaluated the number of pruritic episodes, the type of pruritic behavior and the duration of each pruritic episode in seconds.

Observed pruritic behavior (i.e., licking, biting/chewing, scratching, head shaking, scooting, rolling, pawing, and rubbing) and sleeping was measured using a categorical scoring system 'Yes／no' (i.e. 1 or 0) at 1 min epochs, as previously reported (Gonzales et al., 2016; Gonzales et al., 2013). The number of minutes categorized as 'yes' for each displayed pruritic behavior (i.e., licking, biting/chewing, scratching, head shaking, scooting, rolling, pawing, and rubbing) for an animal was then summed with a maximal achievable score of 300 for the observation period of 300 minutes.

Assessment of global wheal score

As previously described, a global wheal score (GWS) was evaluated at 30 minutes post injections (Banovic et al., 2019; Bizikova et al., 2010). Wheals were measured in two orthogonal directions in millimeters. Erythema and induration were then assigned a score from 1-3 (1=no erythema/flaccid wheal, 2=weak erythema/moderate induration, 3=strong erythema/firm induration). The same investigator evaluated the wheal and

erythema formation and was blinded as to whether CQ or saline had been administered until all data were collected.

Statistical analysis

The evaluation of the pruritic effects and GWS was compared between the vehicle (buffered saline) and CQ. Data were evaluated for normality with a D'Agostino and Pearson omnibus normality test. Depending on the normality test outcome for global wheal scores, IV and intradermal CQ phases, parametric repeated measures ANOVA or the nonparametric alternative, the Friedman test, was utilized. For the data from the SC CQ injections, Wilcoxon matched-pairs signed rank test was applied. All tests were considered significant at $p<0.05$; Bonferroni or Dunn's correction test was used for multiple comparisons between all groups of values depending on the parametric vs. nonparametric test.

Results

Intravenous and subcutaneous chloroquine administration

There were no side effects observed after IV or SC CQ administration in any dog. There was no significant increase in generalized pruritic behavior (pruritic seconds) observed after IV administration of CQ (Figure 3.1a) to healthy beagle dogs during the observation period of 300 minutes (Friedman test; CQ1 vs. saline_01, $P = 0.99$ and CQ1 vs. saline_02, $P = 0.99$; CQ2 vs. saline_01, $P = 0.99$ and CQ2 vs. saline_02, $P = 0.33$). Furthermore, there was no significant itch induction within the 180-300 minutes post-injection (Figure 3.1c; Friedman test; CQ1 vs. saline_01, $P = 0.99$ and CQ1 vs.

saline_02, *P* = 0.66; CQ2 vs. saline_01 and CQ2 vs. saline_02, *P* = 0.99, respectively), which has been previously reported as the peak time of CQ-induced itch in healthy dogs (Aberg et al., 2015).

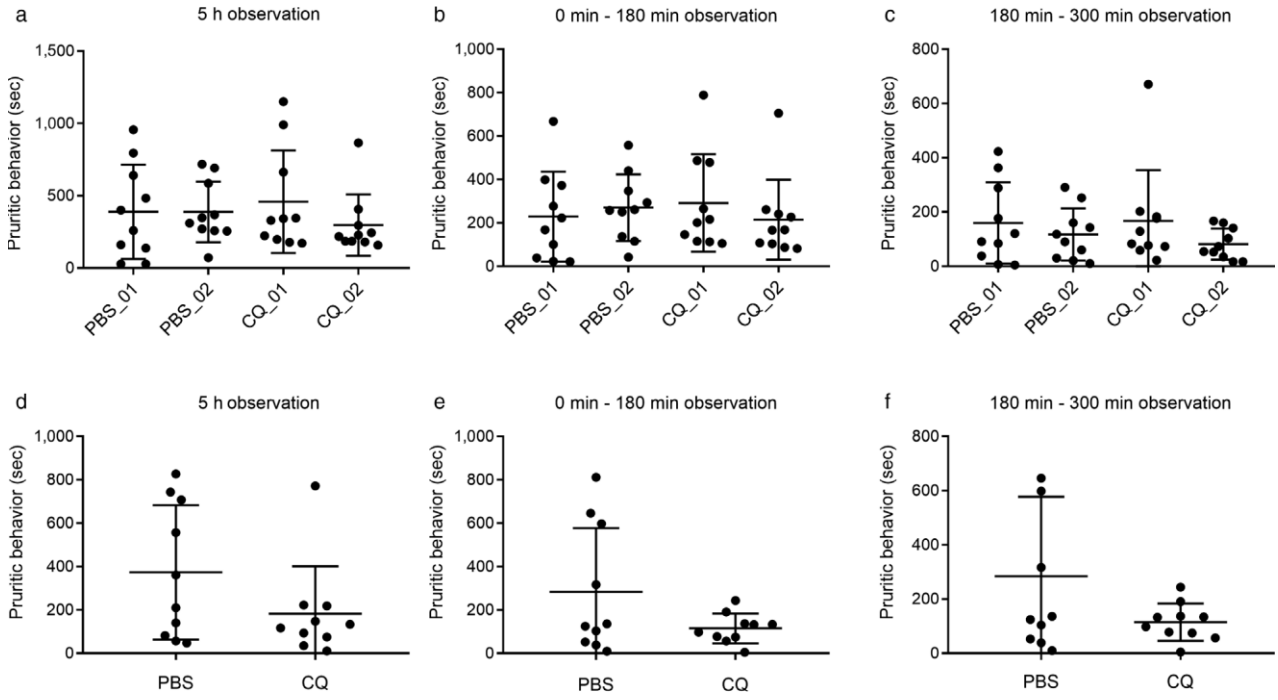

Figure 3.1. Evaluations of pruritic behavior after systemic injections of chloroquine (CQ). No significant increase in generalized pruritic behavior (pruritic seconds and episodes) was observed after intravenous (a, b, c) and subcutaneous (d, e, f) administration of CQ in vivo to purpose-bred healthy beagle dogs during the observation period of 300 min (a, d), 0–180 min (b, e) or 180–300 min (c, f).

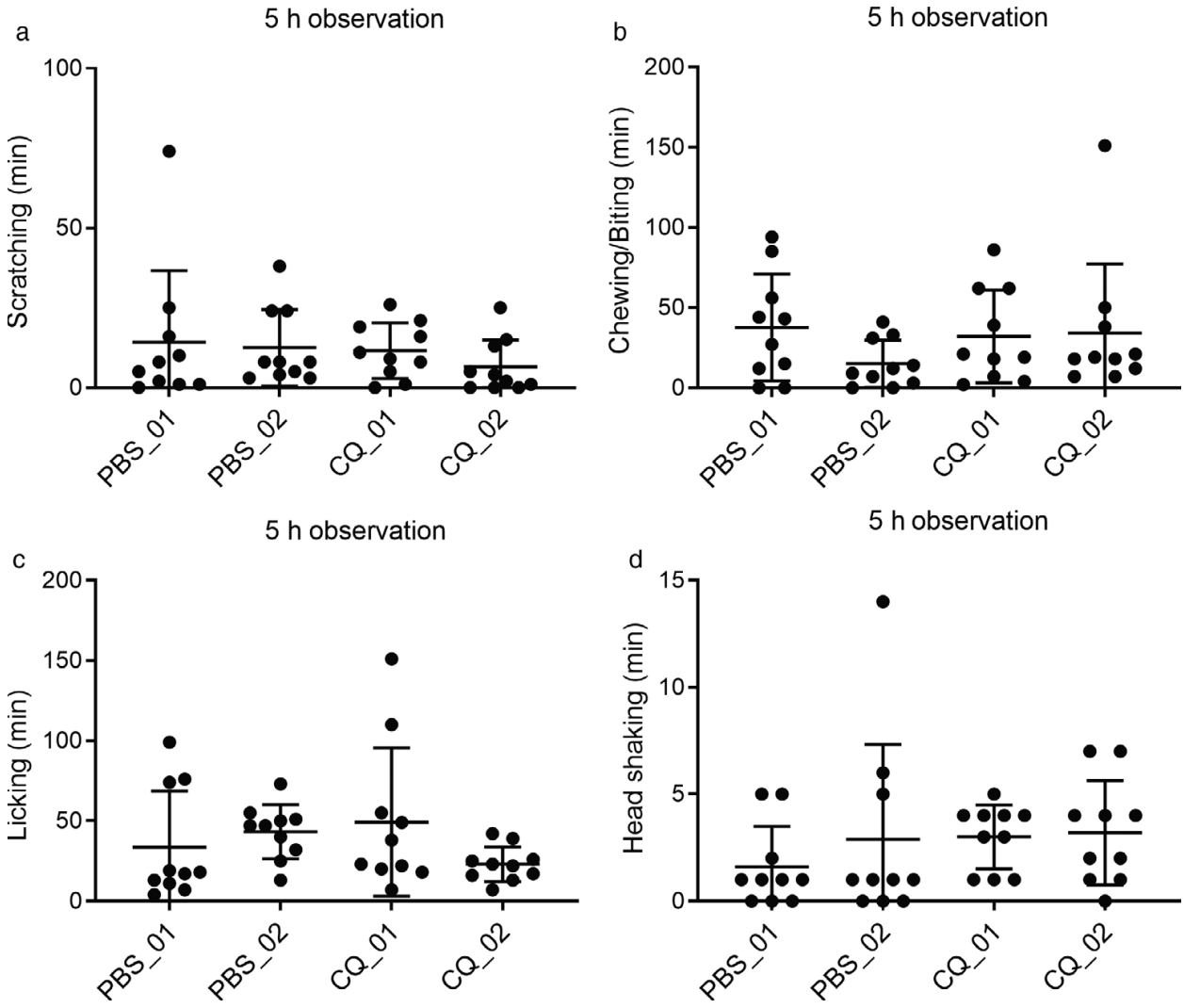

Figure 3.2. Behavioral changes after intravenous chloroquine (CQ) administration. There was no significant increase in any type of pruritic behavior after CQ injection compared to placebo during the observation period of 300 min.

Subcutaneous administration of CQ to healthy dogs did not increase generalized pruritic seconds during 300 minutes (Figure 3.1d; one-tailed Wilcoxon signed rank test; CQ vs. saline_01, $P = 0.08$) or within the 180-300 minutes post-injection (Figure 1f; one-tailed Wilcoxon signed rank test; CQ vs. saline, $P = 0.13$)

The type of generalized pruritic behaviors exhibited during the IV CQ and placebo, were consistent among the healthy dogs; licking, biting/chewing, and scratching were most commonly noted. Intravenous CQ administration did not induce a significant increase in any pruritic behavior compared to placebo during the observation period of 300 minutes (Figure 3.2).

Intradermal chloroquine administration

No episodes of behavior considered to be pain-related were observed in any of the dogs. Intradermal injections of CQ resulted in a positive wheal and erythema reactions in all dogs (Figure 3.3); global wheal scores at 30 min post-injection of each CQ concentration significantly increased compared to saline controls (Figure 3.4a; Friedman test; $P \leq 0.05$).

Figure 3.3. Clinical images of wheal and flare responses following intradermal injections of chloroquine (CQ) and phosphate buffered saline (PBS) control. Intradermal CQ injections at 200 µg/site (a, b) and 400 µg/site (c, d) resulted in a positive wheal and

erythema reactions in all dogs; the PBS control did not induce erythema and wheal reactions (e, f).

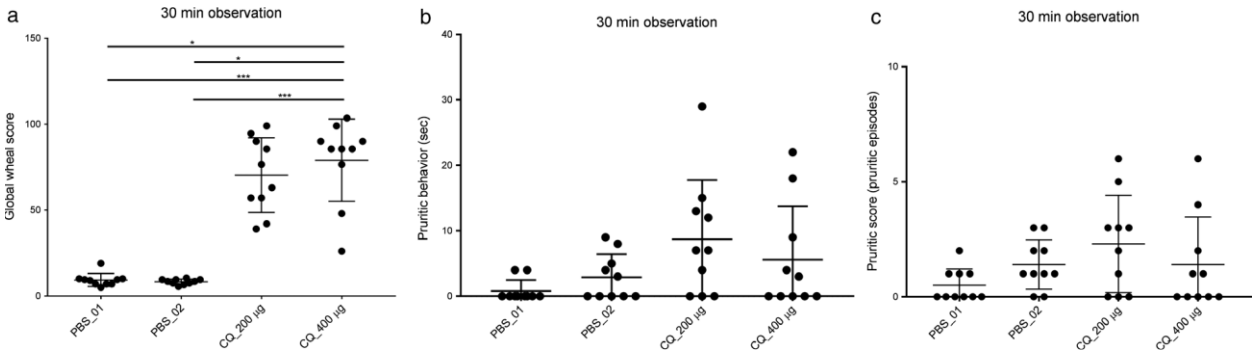

Figure 3.4. Evaluations of global wheal scores (GWS) scores and localized pruritic behaviors after intradermal injections of chloroquine (CQ). (a) The GWS 30 min after CQ injection significantly increased at all concentrations compared to control. (b) Intradermal CQ injections induced mild acute pruritic behaviors at the site of injection of 200 µg and 400 µg CQ in dogs; however, these differences were not statistically significant for the pruritic seconds or episodes for either CQ concentration.

A blinded evaluation revealed that intradermal CQ injections induced mild acute pruritic behaviors in dogs at 200 µg/site and 400 µg/site, respectively, when compared to saline control (Figure 3.4b,c). However, these differences were not statistically significant for the pruritic seconds or episodes for either CQ concentration, 200 µg/site (Friedman test; pruritic seconds, CQ vs. saline_01, $P = 0.06$ and CQ vs. saline_02, $P = 0.90$; pruritic episodes, CQ vs. saline_01, $P = 0.33$ and CQ vs. saline_02, $P = 0.99$) or 400 µg/site

(Friedman test; pruritic seconds, CQ vs. saline_01, $P = 0.15$ and CQ vs. saline_02, $P = 0.99$; pruritic episodes, CQ vs. saline_01 and CQ vs. saline_02, $P = 0.99$, receptively).

Discussion and Conclusions

In this study, CQ was not able to elicit statistically significant pruritic behavior when injected in healthy dogs, regardless of the route of administration. This finding is unlikely to be related to lack of CQ-induced cutaneous inflammation or the tested CQ concentrations. Positive wheal reactions were observed in all dogs included in this study and the injected CQ concentrations were equivalent to those previously used in dogs (Aberg et al., 2015) and mice (Liu et al., 2009) for the investigations of pruritus. Furthermore, our recording period of 300 minutes is identical to the recordings utilized in the previously published canine study which investigated CQ-induced itch in healthy Beagle dogs (Aberg et al., 2015).

The Mrgprs, expressed on peripheral terminals of sensory neurons and mast cells, are implicated in allergic inflammation and itch (Subramanian et al., 2016). In mast cell-deficient mice, CQ induces reduced numbers of scratching bouts compared to wild-type, which suggests that CQ provokes itch independent of mast cell degranulation and the subsequent histamine release (Liu et al., 2009). Chloroquine provokes itch in a histamine-independent manner on skin sensory nerves by activating the Mrgp receptor A3 (MrgprA3) and MrgprX1 in peripheral sensory neurons in rodents and humans, respectively (Akiyama et al., 2010; Liu et al., 2009). A comparison of the Mrgprs repertoires in dog and human revealed that dogs have MrgprX2 and MrgprD, and that

these receptor subsets in the dog genome is more similar to that in humans than rodents (Haitina et al., 2009; Subramanian et al., 2016). Since Mrgpr members are highly homologous to each other (Liu et al., 2009) and the intradermal CQ injections induced wheal responses in our dogs, it is possible that canine MrgprX2 and MrgprD provide the partial physiologic role of rodent MrgprA3 and human MrgprX1. Further investigations are warranted to understand the selectivity of the canine Mrgprs and their selective activation with different pruritogens.

A previous investigation reported that IV and SC administration of CQ induces generalized pruritus in healthy Beagle dogs; licking, biting, and scratching developed within 1 of IV and 20 min after subcutaneous CQ administration (Aberg et al., 2015). Furthermore, it was proposed that CQ-induced itch could be utilized as a model for tests of compounds with potential antipruritic activity in dogs. One can only hypothesize the reason for differences in results in our dogs and the previous study (Aberg et al., 2015). A simple explanation could be the design of the studies and the method of pruritic behaviors evaluation. In rodent models of pruritus, video-recorded pruritic behaviors are blindly evaluated and counted for pruritic episodes and total seconds of itch (Akiyama et al., 2010; Foroutan et al., 2015; Tarrasón, 2017). However, in the prior canine study, different laboratory personnel recorded itch behavior as visual real-time direct observations in the presence of the dogs, and there were no attempts made to record the seconds of itch behavior. Additionally, the pruritic episodes were measured without detailed descriptions for each of the itch behaviors which resulted in scoring variability between evaluators (Aberg et al., 2015). In the study presented here, we used video

recordings to avoid direct attention and influence of evaluators presence on the dog behaviors. Furthermore, our evaluators were blinded to the treatments during video analysis. Another possible explanation for the observed difference in CQ-induced pruritic effect in the other study could be the lack of the baseline pruritus evaluations for all dogs prior to CQ administration. The design of our study included baseline evaluations where each dog serves as its control during treatments; this allows for a minimal effect of individual's variability in pruritic behaviors between dogs and the treatment effect.

Previous studies evaluating pruritus in dogs rarely describe the in-depth methodology regarding the itch behaviors that are scored during the analysis and what type of behaviors are observed (e.g., licking, chewing biting, scratching) (Aberg et al., 2015; Carr et al., 2009; Gonzales et al., 2016; Gonzales et al., 2013; Olivry et al., 2013). Moreover, some studies utilize real-time visual observations by having evaluators directly present near the dogs (Aberg et al., 2015; Olivry et al., 2013). Altogether, the limitations mentioned above lead to differences and inconsistencies between canine pruritus study designs and the results cannot be compared directly. Although the pruritic ethogram presented in this study was developed by collecting data from the previous itch studies in dogs, there is still a need for the validation of the ethogram using an established pruritogen in dogs. It is hoped that the methodology in this study will help establish a framework for future investigations and quantification of itch in dogs.

To the best of the authors' knowledge, we have identified for the first time that intradermal CQ injections can induce wheal and erythema responses in healthy dogs. In contrast to the reported systemic CQ-induced pruritus in healthy dogs, we found no significant pruritic behavior when CQ was injected in our dogs, regardless of the route of administration. We have developed a methodology to quantify systemic pruritus in dogs utilizing ethogram for canine pruritic behaviors and by scoring systemic and local itch behaviors using blinded video-recordings. Since CQ is not considered an agonist of human and murine MrgprX2 and MrgprD which are present in dogs, the role of other Mrgprs agonists in the pathogenesis of canine itch warrants further investigations. Future studies would benefit from assessment of pruritic behaviors in a larger sample size of dogs with different established MrgprX2 (i.e., substance P, compound 48/80) and MrgprD agonists (i.e., beta-alanine).

CHAPTER 6

FINAL CONCLUSIONS AND FUTURE DIRECTIONS

Regarding IgE, the molecular characterization of experimental models utilized to evaluate therapeutics for spontaneous inflammatory skin diseases is essential for future mechanistic and immunomodulatory pre-clinical studies in humans and dogs. In this study, IgE-mediated skin lesions appear to regulate similar T-helper pathways and barrier changes to that of acute spontaneous human AD lesions through examination of the RNA-seq transcriptome; IL-13 represents the dominant Th2 cytokine in this model. Although the initial pilot study using qRT-PCR revealed that prednisolone reduced IL-13, IL-5, CCL2, CCL5 and CCL17 in IgE-mediated skin lesions, further molecular studies using RNA-seq should investigate the effect of established canine anti-allergic drugs (e.g., glucocorticoids, oclacitinib as JAK inhibitor) to validate the canine IgE model.

This is the first study to show that spontaneous canine AD skin has a molecular resemblance to human AD using robust RNA sequencing technology. However, the main constraint of RNA sequencing technology involves limited information regarding the spatial cell diversity and understanding how cells communicate. Future studies in canine AD should focus on capturing gene expression at the individual cell level using single cell RNA sequencing, allowing for a more detailed analysis of cellular diversity. This approach should be able to classify, characterize, and distinguish each cell at the transcriptome level. This could lead to a better understanding of how cell

communication is occurring and allow potential identification of rare cell populations that may be functionally important in the disease.

To our knowledge, this is the first study to show that intradermal CQ injections can induce wheal and erythema responses in healthy dogs. In contrast to the reported systemic CQ-induced pruritus in healthy dogs, we found no significant pruritic behavior when CQ was injected in our dogs, regardless of the route of administration. Using video recordings where the clinical evaluators were blinded to the treatments, we have developed a methodology to quantify systemic and intradermal pruritus in dogs utilizing an ethogram for canine pruritic behaviors and scoring systemic and local itch behaviors. Future studies in dogs are still needed to evaluate the various pruritogens known to induce itch in humans and mice (MRPRX2 agonists, IL-33, IL-31, periostin, etc.). With continued research in this area, it is possible to develop a reliable non-histaminergic canine model of pruritus that can be used to evaluate novel anti-pruritic drugs in dogs and humans.

REFERENCES

Aberg, G.A., Arulnesan, N., Bolger, G.T., Ciofalo, V.B., Pucaj, K., 2015. Characterization and Validation of a Canine Pruritic Model. Drug Dev Res 76, 246-250.

Abila, B., Ezeamuzie, I.C., Igbigbi, P.S., Ambakederemo, A.W., Asomugha, L., 1994. Effects of two antihistamines on chloroquine and histamine induced weal and flare in healthy African volunteers. Afr J Med Med Sci 23, 139-142.

Aderounmu, A.F., Fleckenstein, L., 1983. Pharmacokinetics of chloroquine diphosphate in the dog. J Pharmacol Exp Ther 226, 633-639.

Ajayi, A., Oluokun, A;, Sofowora, O;, Akimleye, A.;Ajayi, A.T., 1989. Epidemiology of antimalarial- induced pruritis in Africans. Eur J Clin Pharmacol.

Akiyama, T., Carstens, M.I., Carstens, E., 2010. Differential itch- and pain-related behavioral responses and micro-opoid modulation in mice. Acta Derm Venereol 90, 575-581.

Akiyama, T., Lerner, E.A., Carstens, E., 2015. Protease-activated receptors and itch. Handb Exp Pharmacol 226, 219-235.

Anders, S., Pyl, P.T., Huber, W., 2015. HTSeq--a Python framework to work with high-throughput sequencing data. Bioinformatics 31, 166-169.

Andrews, S., 2010. FastQC: A quality control tool for high throughput sequence data, 0.11.8 ed. Babraham Bioinformatics.

Arai, I., Tsuji, M., Miyagawa, K., Takeda, H., Akiyama, N., Saito, S., 2014. Increased itching sensation depend on an increase in the dorsal root ganglia IL-31 receptor A (IL-31RA) expression in mice with atopic-dermatitis. Itch & Pain 1, e467.

Banovic, F., Denley, T., Blubaugh, A., 2019. Dose-dependent pruritogenic and inflammatory effects of intradermal injections of histamine, compound 48/80 and anti-canine IgE in healthy dogs. Vet Dermatol 30, 325-e391.

Banovic, F., Denley, T., Blubaugh, A., Scheibe, I., Lemo, N., Papich, M.G., 2020. Effect of diphenhydramine and cetirizine on immediate and late-phase cutaneous allergic reactions in healthy dogs: a randomized, double-blinded crossover study. Vet Dermatol 31, 256-e258.

Baumer, W., Rossbach, K., Schmidt, B.H., 2017. The selective glucocorticoid receptor agonist mapracorat displays a favourable safety-efficacy ratio for the topical treatment of inflammatory skin diseases in dogs. Vet Dermatol 28, 46-e11.

Bieber, T., 2014. Insights into immunoglobulin E-mediated late-phase reactions in dogs. Vet Dermatol 25, 305-306.

Bieber, T., 2020. Interleukin-13: Targeting an underestimated cytokine in atopic dermatitis. Allergy 75, 54-62.

Bieber, T., D'Erme, A.M., Akdis, C.A., Traidl-Hoffmann, C., Lauener, R., Schappi, G., Schmid-Grendelmeier, P., 2017. Clinical phenotypes and endophenotypes of atopic dermatitis: Where are we, and where should we go? J Allergy Clin Immunol 139, S58-S64.

Bizikova, P., Linder, K.E., Paps, J., Olivry, T., 2010. Effect of a novel topical diester glucocorticoid spray on immediate- and late-phase cutaneous allergic reactions in Maltese-beagle atopic dogs: a placebo-controlled study. Vet Dermatol 21, 70-79.

Blubaugh, A., Rissi, D., Elder, D., Denley, T., Eguiluz-Hernandez, S., Banovic, F., 2018. The anti-inflammatory effect of topical tofacitinib on immediate and late-phase cutaneous allergic reactions in dogs: a placebo-controlled pilot study. Vet Dermatol 29, 250-e293.

Bolger, A.M., Lohse, M., Usadel, B., 2014. Trimmomatic: a flexible trimmer for Illumina sequence data. Bioinformatics 30, 2114-2120.

Carr, M.N., Torres, S.M., Koch, S.N., Reiter, L.V., 2009. Investigation of the pruritogenic effects of histamine, serotonin, tryptase, substance P and interleukin-2 in healthy dogs. Vet Dermatol 20, 105-110.

Clark, R.A., 1989. Cell-mediated and IgE-mediated immune responses in atopic dermatitis. Arch Dermatol 125, 413-416.

Daehwan, K., Pertea, G.;, Trapnell, C.;, et al., 2013. TopHat2: accurate alignment of transcriptomes in the presence of insertions, deletions, and gene fusions. Genome Biol.

Esaki, H., Brunner, P.M., Renert-Yuval, Y., Czarnowicki, T., Huynh, T., Tran, G., Lyon, S., Rodriguez, G., Immaneni, S., Johnson, D.B., Bauer, B., Fuentes-Duculan, J., Zheng, X., Peng, X., Estrada, Y.D., Xu, H., de Guzman Strong, C., Suarez-Farinas, M., Krueger, J.G., Paller, A.S., Guttman-Yassky, E., 2016. Early-onset pediatric atopic dermatitis is T(H)2 but also T(H)17 polarized in skin. J Allergy Clin Immunol 138, 1639-1651.

Esaki, H., Ewald, D.A., Ungar, B., Rozenblit, M., Zheng, X., Xu, H., Estrada, Y.D., Peng, X., Mitsui, H., Litman, T., Suarez-Farinas, M., Krueger, J.G., Guttman-Yassky, E., 2015. Identification of novel immune and barrier genes in atopic dermatitis by means of laser capture microdissection. J Allergy Clin Immunol 135, 153-163.

Ewald, D.A., Malajian, D., Krueger, J.G., Workman, C.T., Wang, T., Tian, S., Litman, T., Guttman-Yassky, E., Suarez-Farinas, M., 2015. Meta-analysis derived atopic dermatitis

(MADAD) transcriptome defines a robust AD signature highlighting the involvement of atherosclerosis and lipid metabolism pathways. BMC Med Genomics 8, 60.

Ewald, D.A., Noda, S., Oliva, M., Litman, T., Nakajima, S., Li, X., Xu, H., Workman, C.T., Scheipers, P., Svitacheva, N., Labuda, T., Krueger, J.G., Suarez-Farinas, M., Kabashima, K., Guttman-Yassky, E., 2017. Major differences between human atopic dermatitis and murine models, as determined by using global transcriptomic profiling. J Allergy Clin Immunol 139, 562-571.

Eyerich, K., Novak, N., 2013. Immunology of atopic eczema: overcoming the Th1/Th2 paradigm. Allergy 68, 974-982.

Foroutan, A., Haddadi, N.S., Ostadhadi, S., Sistany, N., Dehpour, A.R., 2015. Chloroquine-induced scratching is mediated by NO/cGMP pathway in mice. Pharmacol Biochem Behav 134, 79-84.

Freudenberg, J.M., Olivry, T., Mayhew, D.N., Rubenstein, D.S., Rajpal, D.K., 2019. The Comparison of Skin Transcriptomes Confirms Canine Atopic Dermatitis Is a Natural Homologue to the Human Disease. J Invest Dermatol 139, 968-971.

Furue, M., Kadono, T., 2015. New therapies for controlling atopic itch. J Dermatol 42, 847-850.

Gittler, J.K., Krueger, J.G., Guttman-Yassky, E., 2013. Atopic dermatitis results in intrinsic barrier and immune abnormalities: implications for contact dermatitis. J Allergy Clin Immunol 131, 300-313.

Gittler, J.K., Shemer, A., Suarez-Farinas, M., Fuentes-Duculan, J., Gulewicz, K.J., Wang, C.Q., Mitsui, H., Cardinale, I., de Guzman Strong, C., Krueger, J.G., Guttman-Yassky, E., 2012. Progressive activation of T(H)2/T(H)22 cytokines and selective epidermal proteins characterizes acute and chronic atopic dermatitis. J Allergy Clin Immunol 130, 1344-1354.

Gonzales, A.J., Fleck, T.J., Humphrey, W.R., Galvan, B.A., Aleo, M.M., Mahabir, S.P., Tena, J.K., Greenwood, K.G., McCall, R.B., 2016. IL-31-induced pruritus in dogs: a novel experimental model to evaluate anti-pruritic effects of canine therapeutics. Vet Dermatol 27, 34-e10.

Gonzales, A.J., Humphrey, W.R., Messamore, J.E., Fleck, T.J., Fici, G.J., Shelly, J.A., Teel, J.F., Bammert, G.F., Dunham, S.A., Fuller, T.E., McCall, R.B., 2013. Interleukin-31: its role in canine pruritus and naturally occurring canine atopic dermatitis. Vet Dermatol 24, 48-53 e11-42.

Grobe, W., Bieber, T., Novak, N., 2019. Pathophysiology of atopic dermatitis. J Dtsch Dermatol Ges 17, 433-440.

Guttman-Yassky, E., Diaz, A., Pavel, A.B., Fernandes, M., Lefferdink, R., Erickson, T., Canter, T., Rangel, S., Peng, X., Li, R., Estrada, Y., Xu, H., Krueger, J.G., Paller, A.S., 2019. Use of Tape Strips to Detect Immune and Barrier Abnormalities in the Skin of Children With Early-Onset Atopic Dermatitis. JAMA Dermatol 155, 1358-1370.

Haitina, T., Fredriksson, R., Foord, S.M., Schioth, H.B., Gloriam, D.E., 2009. The G protein-coupled receptor subset of the dog genome is more similar to that in humans than rodents. BMC Genomics 10, 24.

Hamilton, J.D., Suarez-Farinas, M., Dhingra, N., Cardinale, I., Li, X., Kostic, A., Ming, J.E., Radin, A.R., Krueger, J.G., Graham, N., Yancopoulos, G.D., Pirozzi, G., Guttman-Yassky, E., 2014. Dupilumab improves the molecular signature in skin of patients with moderate-to-severe atopic dermatitis. J Allergy Clin Immunol 134, 1293-1300.

Hanzelmann, S., ; Castelo, R,; Guinney, J., 2015. GSVA: gene set variation analysis for microarray and RNA-Seq data. BMC Bioinformatics 14, 1471-2105.

Hensel, P., Santoro, D., Favrot, C., Hill, P., Griffin, C., 2015. Canine atopic dermatitis: detailed guidelines for diagnosis and allergen identification. BMC Vet Res 11, 196.

Hensel, P., Saridomichelakis, M., Eisenschenk, M., Tamamoto-Mochizuki, C., Pucheu-Haston, C., Santoro, D., International Committee on Allergic Diseases of, A., 2024. Update on the role of genetic factors, environmental factors and allergens in canine atopic dermatitis. Vet Dermatol 35, 15-24.

Hofker, M.H., Fu, J., Wijmenga, C., 2014. The genome revolution and its role in understanding complex diseases. Biochim Biophys Acta 1842, 1889-1895.

Jassies-van der Lee, A., Rutten, V.P., Bruijn, J., Willemse, T., Broere, F., 2014. CD4+ and CD8+ skin-associated T lymphocytes in canine atopic dermatitis produce interleukin-13, interleukin-22 and interferon-gamma and contain a CD25+ FoxP3+ subset. Vet Dermatol 25, 456-e472.

Jin, H., He, R., Oyoshi, M., Geha, R.S., 2009. Animal models of atopic dermatitis. J Invest Dermatol 129, 31-40.

Kubo, T., Sato, S., Hida, T., Minowa, T., Hirohashi, Y., Tsukahara, T., Kanaseki, T., Murata, K., Uhara, H., Torigoe, T., 2021. IL-13 modulates ΔNp63 levels causing altered expression of barrier- and inflammation-related molecules in human keratinocytes: A possible explanation for chronicity of atopic dermatitis. Immun Inflamm Dis 9, 734-745.

Kunimura, K., Fukui, Y., 2021. The molecular basis for IL-31 production and IL-31-mediated itch transmission: from biology to drug development. Int Immunol 33, 731-736.

LaMotte, R.H., Shimada, S.G., Sikand, P., 2011. Mouse models of acute, chemical itch and pain in humans. Exp Dermatol 20, 778-782.

Lee, J., Park, C.O., Lee, K.H., 2015. Specific immunotherapy in atopic dermatitis. Allergy Asthma Immunol Res 7, 221-229.

Leung, D.Y., Bhan, A.K., Schneeberger, E.E., Geha, R.S., 1983. Characterization of the mononuclear cell infiltrate in atopic dermatitis using monoclonal antibodies. J Allergy Clin Immunol 71, 47-56.

Liu, Q., Tang, Z., Surdenikova, L., Kim, S., Patel, K.N., Kim, A., Ru, F., Guan, Y., Weng, H.J., Geng, Y., Undem, B.J., Kollarik, M., Chen, Z.F., Anderson, D.J., Dong, X., 2009. Sensory neuron-specific GPCR Mrgprs are itch receptors mediating chloroquine-induced pruritus. Cell 139, 1353-1365.

Livak, K.J., Schmittgen, T.D., 2001. Analysis of relative gene expression data using real-time quantitative PCR and the 2(-Delta Delta C(T)) Method. Methods 25, 402-408.

Lourenco, A.M., Schmidt, V., Sao Braz, B., Nobrega, D., Nunes, T., Duarte-Correia, J.H., Matias, D., Maruhashi, E., Reme, C.A., Nuttall, T., 2016. Efficacy of proactive long-term maintenance therapy of canine atopic dermatitis with 0.0584% hydrocortisone aceponate spray: a double-blind placebo controlled pilot study. Vet Dermatol 27, 88-92e25.

Love, M.I., Huber, W., Anders, S., 2014. Moderated estimation of fold change and dispersion for RNA-seq data with DESeq2. Genome Biol 15, 550.

Marsalla, R., Girolomoni G., 2009. Canine models of Atopic Dermatitis: a Useful Tool with Untapped Potential. Journal of Investigative Dermatology, 2351-2357.

Marsella, R., 2021. Advances in our understanding of canine atopic dermatitis. Vet Dermatol 32, 547-e151.

Marsella, R., De Benedetto, A., 2017. Atopic Dermatitis in Animals and People: An Update and Comparative Review. Vet Sci 4.

Martel, B.C., Lovato, P., Baumer, W., Olivry, T., 2017. Translational Animal Models of Atopic Dermatitis for Preclinical Studies. Yale J Biol Med 90, 389-402.

Matucci, A., Maggi, E., Vultaggio, A., 2019. Eosinophils, the IL-5/IL-5Ralpha axis, and the biologic effects of benralizumab in severe asthma. Respir Med 160, 105819.

Metacore, 2023. Metacore, a Cortellis solution, © 2022 Clarivate. https://clarivate.com/cortellis/solutions/early-research-intelligence-solutions/ (accessed February 8 2023).

Mikhaylov, D., Del Duca, E., Guttman-Yassky, E., 2021. Proteomic signatures of inflammatory skin diseases: a focus on atopic dermatitis. Expert Rev Proteomics 18, 345-361.

Mollanazar, N.K., Smith, P.K., Yosipovitch, G., 2016. Mediators of Chronic Pruritus in Atopic Dermatitis: Getting the Itch Out? Clin Rev Allergy Immunol 51, 263-292.

Nomura, T., Honda, T., Kabashima, K., 2018. Multipolarity of cytokine axes in the pathogenesis of atopic dermatitis in terms of age, race, species, disease stage and biomarkers. Int Immunol 30, 419-428.

Olivry, T., 2012. What Can Dogs Bring to Atopic Dermatitis Research? Chem Immunol Allergy 96, 61-72.

Olivry, T., Baeumer, W., 2017. Treatment of itch in dogs: a mechanistic approach. Veterinary Dermatology VDE 2017, 63-70.

Olivry, T., Bizikova, P., Paps, J.S., Dunston, S., Lerner, E.A., Yosipovitch, G., 2013. Cowhage can induce itch in the atopic dog. Exp Dermatol 22, 435-437.

Olivry, T., DeBoer, D.J., Favrot, C., Jackson, H.A., Mueller, R.S., Nuttall, T., Prelaud, P., International Committee on Allergic Diseases of, A., 2015. Treatment of canine atopic dermatitis: 2015 updated guidelines from the International Committee on Allergic Diseases of Animals (ICADA). BMC Vet Res 11, 210.

Olivry, T., Dunston, S.M., Murphy, K.M., Moore, P.F., 2001. Characterization of the inflammatory infiltrate during IgE-mediated late phase reactions in the skin of normal and atopic dogs. Vet Dermatol 12, 49-58.

Olivry, T., Hill, P.B., 2001. The ACVD task force on canine atopic dermatitis (XVIII): histopathology of skin lesions. Vet Immunol Immunopathol 81, 305-309.

Olivry, T., Mayhew, D., Paps, J.S., Linder, K.E., Peredo, C., Rajpal, D., Hofland, H., Cote-Sierra, J., 2016. Early Activation of Th2/Th22 Inflammatory and Pruritogenic Pathways in Acute Canine Atopic Dermatitis Skin Lesions. J Invest Dermatol 136, 1961-1969.

Osifo, N.G., 1991. Structure activity relationships in the pruritogenicity of chloroquine and amodiaquine metabolites in a dog model. J Dermatol Sci 2, 92-96.

Paps, J.S., Baumer, W., Olivry, T., 2016. Development of an Allergen-induced Atopic Itch Model in Dogs: A Preliminary Report. Acta Derm Venereol 96, 400-401.

Pearson, J., Leon, R., Starr, H., Kim, S.J., Fogle, J.E., Banovic, F., 2023. Establishment of an Intradermal Canine IL-31-Induced Pruritus Model to Evaluate Therapeutic Candidates in Atopic Dermatitis. Vet Sci 10.

Plager, D.A., Torres, S.M., Koch, S.N., Kita, H., 2012. Gene transcription abnormalities in canine atopic dermatitis and related human eosinophilic allergic diseases. Vet Immunol Immunopathol 149, 136-142.

Plant, J.D., Neradilek, M.B., 2017. Effectiveness of regionally-specific immunotherapy for the management of canine atopic dermatitis. BMC Vet Res 13, 4.

Pucheu-Haston, C.M., Bizikova, P., Marsella, R., Santoro, D., Nuttall, T., Eisenschenk, M.N., 2015. Review: Lymphocytes, cytokines, chemokines and the T-helper 1-T-helper 2 balance in canine atopic dermatitis. Vet Dermatol 26, 124-e132.

Pucheu-Haston, C.M., Kasparek, K.A., Stout, R.W., Kearney, M.T., Hammerberg, B., 2014. Effects of pentoxifylline on immediate and late-phase cutaneous reactions in response to anti-immunoglobulin E antibodies in clinically normal dogs. Am J Vet Res 75, 152-160.

Pucheu-Haston, C.M., Shuster, D., Olivry, T., Brianceau, P., Lockwood, P., McClanahan, T., de Waal Malefyt, R., Mattson, J.D., Hammerberg, B., 2006. A canine model of cutaneous late-phase reactions: prednisolone inhibition of cellular and cytokine responses. Immunology 117, 177-187.

Rerknimitr, P., Otsuka, A., Nakashima, C., Kabashima, K., 2017. The etiopathogenesis of atopic dermatitis: barrier disruption, immunological derangement, and pruritus. Inflamm Regen 37, 14.

Ritchie, M.E., Phipson, B., Wu, D., Hu, Y., Law, C.W., Shi, W., Smyth, G.K., 2015. limma powers differential expression analyses for RNA-sequencing and microarray studies. Nucleic Acids Res 43, e47.

Roduit, C., Frei, R., Depner, M., Karvonen, A.M., Renz, H., Braun-Fahrlander, C., Schmausser-Hechfellner, E., Pekkanen, J., Riedler, J., Dalphin, J.C., von Mutius, E., Lauener, R.P., the, P.s.g., Hyvarinen, A., Kirjavainen, P., Remes, S., Roponen, M., Dalphin, M.L., Kaulek, V., Ege, M., Genuneit, J., Illi, S., Kabesch, M., Schaub, B., Pfefferle, P.I., Doekes, G., 2017. Phenotypes of Atopic Dermatitis Depending on the Timing of Onset and Progression in Childhood. JAMA Pediatr 171, 655-662.

Rozenblit, M., Suarez-Farinas, M., Shemer, A., Khattri, S., Gilleaudeau, P., Sullivan-Whalen, M., Zheng, X., Xu, H., Cardinale, I., Krueger, J.G., Guttman-Yassky, E., 2014. Residual genomic profile after cyclosporine treatment may offer insights into atopic dermatitis reoccurrence. J Allergy Clin Immunol 134, 955-957.

Saaf, A.M., Tengvall-Linder, M., Chang, H.Y., Adler, A.S., Wahlgren, C.F., Scheynius, A., Nordenskjold, M., Bradley, M., 2008. Global expression profiling in atopic eczema reveals reciprocal expression of inflammatory and lipid genes. PLoS One 3, e4017.

Santoro, D., Marsella, R., 2014. Animal Models of Allergic Diseases. Veterinary Sciences 1, 192-212.

Santoro, D., Saridomichelakis, M., Eisenschenk, M., Tamamoto-Mochizuki, C., Hensel, P., Pucheu-Haston, C., International Committee on Allergic Diseases of, A., 2024. Update on the skin barrier, cutaneous microbiome and host defence peptides in canine atopic dermatitis. Vet Dermatol 35, 5-14.

Sanyal, R.D., Pavel, A.B., Glickman, J., Chan, T.C., Zheng, X., Zhang, N., Cueto, I., Peng, X., Estrada, Y., Fuentes-Duculan, J., Alexis, A.F., Krueger, J.G., Guttman-Yassky, E., 2019. Atopic dermatitis in African American patients is T(H)2/T(H)22-skewed with T(H)1/T(H)17 attenuation. Ann Allergy Asthma Immunol 122, 99-110 e116.

Schamber, P., Schwab-Richards, R., Bauersachs, S., Mueller, R.S., 2014. Gene expression in the skin of dogs sensitized to the house dust mite Dermatophagoides farinae. G3 (Bethesda) 4, 1787-1795.

Schlotter, Y.M., Veenhof, E.Z., Brinkhof, B., Rutten, V.P., Spee, B., Willemse, T., Penning, L.C., 2009. A GeNorm algorithm-based selection of reference genes for quantitative real-time PCR in skin biopsies of healthy dogs and dogs with atopic dermatitis. Vet Immunol Immunopathol 129, 115-118.

Steinhoff, M., Ahmad, F., Pandey, A., Datsi, A., AlHammadi, A., Al-Khawaga, S., Al-Malki, A., Meng, J., Alam, M., Buddenkotte, J., 2022. Neuroimmune communication regulating pruritus in atopic dermatitis. J Allergy Clin Immunol 149, 1875-1898.

Suarez-Farinas, M., Dhingra, N., Gittler, J., Shemer, A., Cardinale, I., de Guzman Strong, C., Krueger, J.G., Guttman-Yassky, E., 2013a. Intrinsic atopic dermatitis shows

similar TH2 and higher TH17 immune activation compared with extrinsic atopic dermatitis. J Allergy Clin Immunol 132, 361-370.

Suarez-Farinas, M., Gittler, J.K., Shemer, A., Cardinale, I., Krueger, J.G., Guttman-Yassky, E., 2013b. Residual genomic signature of atopic dermatitis despite clinical resolution with narrow-band UVB. J Allergy Clin Immunol 131, 577-579.

Suarez-Farinas, M., Tintle, S.J., Shemer, A., Chiricozzi, A., Nograles, K., Cardinale, I., Duan, S., Bowcock, A.M., Krueger, J.G., Guttman-Yassky, E., 2011. Nonlesional atopic dermatitis skin is characterized by broad terminal differentiation defects and variable immune abnormalities. J Allergy Clin Immunol 127, 954-964 e951-954.

Suarez-Farinas, M., Ungar, B., Correa da Rosa, J., Ewald, D.A., Rozenblit, M., Gonzalez, J., Xu, H., Zheng, X., Peng, X., Estrada, Y.D., Dillon, S.R., Krueger, J.G., Guttman-Yassky, E., 2015. RNA sequencing atopic dermatitis transcriptome profiling provides insights into novel disease mechanisms with potential therapeutic implications. J Allergy Clin Immunol 135, 1218-1227.

Subramanian, H., Gupta, K., Ali, H., 2016. Roles of Mas-related G protein-coupled receptor X2 on mast cell-mediated host defense, pseudoallergic drug reactions, and chronic inflammatory diseases. J Allergy Clin Immunol 138, 700-710.

Tamamoto-Mochizuki, C., Olivry, T., 2021. IL-31 and IL-31 receptor expression in acute experimental canine atopic dermatitis skin lesions. Vet Dermatol 32, 631-e169.

Tarrasón, G., Carcasona, C.;, Eichhorn, P.;, Perez, B., 2017. Characterization of the mouse model of chloroquine-induced mouse model of pruritus using an automated behavioral system. Experimental Dermatology, 1-7.

Tsoi, L.C., Rodriguez, E., Degenhardt, F., Baurecht, H., Wehkamp, U., Volks, N., Szymczak, S., Swindell, W.R., Sarkar, M.K., Raja, K., Shao, S., Patrick, M., Gao, Y., Uppala, R., Perez White, B.E., Getsios, S., Harms, P.W., Maverakis, E., Elder, J.T.,

Franke, A., Gudjonsson, J.E., Weidinger, S., 2019. Atopic Dermatitis Is an IL-13-Dominant Disease with Greater Molecular Heterogeneity Compared to Psoriasis. J Invest Dermatol 139, 1480-1489.

Tsoi, L.C., Rodriguez, E., Stolzl, D., Wehkamp, U., Sun, J., Gerdes, S., Sarkar, M.K., Hubenthal, M., Zeng, C., Uppala, R., Xing, X., Thielking, F., Billi, A.C., Swindell, W.R., Shefler, A., Chen, J., Patrick, M.T., Harms, P.W., Kahlenberg, J.M., Perez White, B.E., Maverakis, E., Gudjonsson, J.E., Weidinger, S., 2020. Progression of acute-to-chronic atopic dermatitis is associated with quantitative rather than qualitative changes in cytokine responses. J Allergy Clin Immunol 145, 1406-1415.

Turner, M.J., Zhou, B., 2014. A new itch to scratch for TSLP. Trends Immunol 35, 49-50.

Vogelnest, L.J.M., Ralf S.; Dart, Christina M., 2008. The suitability of medetomidine sedation for intradermal skin testing in dogs. Vet Dermatol 11.

Wang, C., Gong, B., Bushel, P.R., Thierry-Mieg, J., Thierry-Mieg, D., Xu, J., Fang, H., Hong, H., Shen, J., Su, Z., Meehan, J., Li, X., Yang, L., Li, H., Labaj, P.P., Kreil, D.P., Megherbi, D., Gaj, S., Caiment, F., van Delft, J., Kleinjans, J., Scherer, A., Devanarayan, V., Wang, J., Yang, Y., Qian, H.R., Lancashire, L.J., Bessarabova, M., Nikolsky, Y., Furlanello, C., Chierici, M., Albanese, D., Jurman, G., Riccadonna, S., Filosi, M., Visintainer, R., Zhang, K.K., Li, J., Hsieh, J.H., Svoboda, D.L., Fuscoe, J.C., Deng, Y., Shi, L., Paules, R.S., Auerbach, S.S., Tong, W., 2014. The concordance between RNA-seq and microarray data depends on chemical treatment and transcript abundance. Nat Biotechnol 32, 926-932.

Wilson, S.R., The, L., Batia, L.M., Beattie, K., Katibah, G.E., McClain, S.P., Pellegrino, M., Estandian, D.M., Bautista, D.M., 2013. The epithelial cell-derived atopic dermatitis cytokine TSLP activates neurons to induce itch. Cell 155, 285-295.

Wollenberg, A., Thomsen, S.F., Lacour, J.P., Jaumont, X., Lazarewicz, S., 2021. Targeting immunoglobulin E in atopic dermatitis: A review of the existing evidence. World Allergy Organ J 14, 100519.

Wood, S.H., Clements, D.N., Ollier, W.E., Nuttall, T., McEwan, N.A., Carter, S.D., 2009. Gene expression in canine atopic dermatitis and correlation with clinical severity scores. J Dermatol Sci 55, 27-33.

Yosipovitch, G., Rosen, J.D., Hashimoto, T., 2018. Itch: From mechanism to (novel) therapeutic approaches. J Allergy Clin Immunol 142, 1375-1390.

Zhang, Y., Parmigiani, G., Johnson, W.E., 2020. ComBat-seq: batch effect adjustment for RNA-seq count data. NAR Genom Bioinform 2, lqaa078.

Zhang, Z., Schwartz, S., Wagner, L., Miller, W., 2000. A greedy algorithm for aligning DNA sequences. J Comput Biol 7, 203-214.